

UNIVERSITY OF NAPLES FEDERICO II

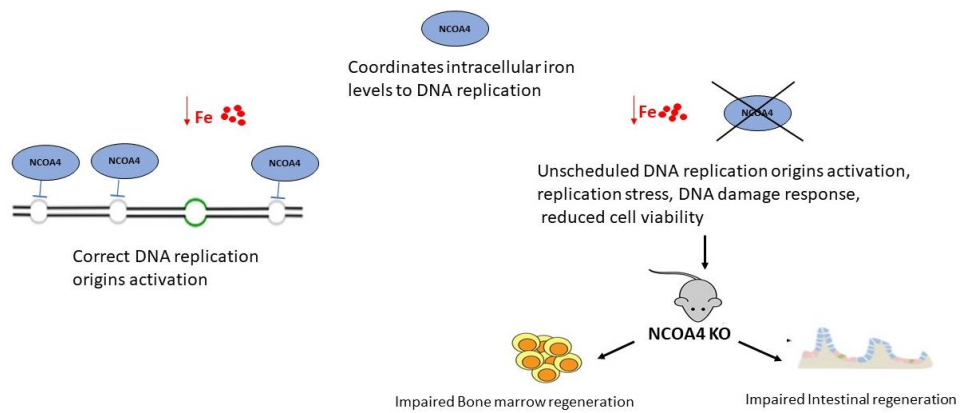
DOCTORATE IN  
MOLECULAR MEDICINE AND MEDICAL BIOTECHNOLOGY

XXXIII CYCLE



Federica Carrillo

**“Relevance of NCOA4 functions in tissue regeneration”**



Year 2021

**UNIVERSITY OF NAPLES FEDERICO II**

**DOCTORATE IN**  
**MOLECULAR MEDICINE AND MEDICAL BIOTECHNOLOGY**

**XXXIII CYCLE**



**“Relevance of NCOA4 functions in tissue regeneration”**

Tutor  
Prof.ssa Francesca Carlomagno

Candidate  
Federica Carrillo

**Year 2021**

## Summary

<b>1. INTRODUCTION</b> .....	6
<b>1.1 The essential role of iron in cellular biology</b> .....	6
<b>1.2 Iron uptake</b> .....	6
<b>1.3 Iron distribution</b> .....	7
<b>1.4 Regulation of iron homeostasis</b> .....	8
<b>1.5 The role of iron in erythropoiesis</b> .....	12
<b>1.6 The role of iron in cell cycle progression</b> .....	12
<b>1.7 The Nuclear Receptor Co-Activator 4</b> .....	15
<b>1.8 NCOA4 regulates Ferritinophagy</b> .....	16
<b>1.9 NCOA4 blocks DNA replication origins activation</b> .....	18
<b>1.10 NCOA4 acts as DNA replication regulator upon iron deprivation</b> .....	20
<b>2. AIM OF THE STUDY</b> .....	22
<b>3. MATERIALS AND METHODS</b> .....	23
<b>3.1 Cell culture</b> .....	23
<b>3.2 Generation of stable clones silenced for NCOA4 protein</b> .....	23
<b>3.3 Labile Iron Pool (LIP) evaluation</b> .....	23
<b>3.4 Protein extraction</b> .....	23
<b>3.5 Hystology Analysis</b> .....	24
<b>3.6 Sodium Dextran Sulfate treatment</b> .....	25
<b>3.7 Rna Extraction and RT-PCR</b> .....	25
<b>3.8 Evaluation of serum Transferrin saturation</b> .....	26
<b>3.9 5- Fluorouracil treatment</b> .....	26
<b>3.10 Colony-forming unit assay</b> .....	26
<b>3.11 Survival experiment</b> .....	26
<b>3.12 Statistical analysis</b> .....	27
<b>4. RESULTS</b> .....	28
<b>4.1 Genetic inactivation of NCOA4 impairs colon regeneration in mice</b> .....	28
<b>4.2 NCOA4 KO mice exhibited defective intestinal stem cells     proliferation</b> .....	33
<b>4.3 NCOA4 KO mice show a low survival after DSS 4% treatment</b> .....	35
<b>4.4 NCOA4 KO mice displayed impaired BM-derived cell proliferation</b> .....	36

<b>4.5 NCOA4 KO BM-derived cells and mice are sensitive to 5-FU treatment compared to WT cells and animals.....</b>	<b>38</b>
<b>4.6 NCOA4 KO mice impaired tissue regeneration is not improved by iron supply .....</b>	<b>41</b>
<b>4.7 The absence of NCOA4 in low iron condition did not affect Iron-Sulfur (Fe-S) cluster proteins levels.....</b>	<b>46</b>
<b>5. DISCUSSION .....</b>	<b>50</b>
<b>6. CONCLUSIONS .....</b>	<b>53</b>
<b>References .....</b>	<b>54</b>

## ABSTRACT

Iron is an essential microelement for DNA replication since it acts as a cofactor for several enzymes involved in DNA metabolism such as DNA polymerases, DNA primases and Ribonucleotide Reductase. Indeed, cells tightly control intracellular iron levels and upon low iron condition they arrest cell cycle avoiding S phase entry and DNA replication.

The Nuclear Receptor CoActivator 4 (NCOA4) has been described as a novel regulator of iron homeostasis that upon low iron conditions controls intracellular iron levels by promoting lysosomal ferritin degradation (Ferritinophagy). Moreover, NCOA4 also acts as a negative regulator of DNA replication by inhibiting DNA replication origin activation via its interaction with MCM7 protein, a component of the MCM2-7 complex which represents the processive helicase of the replication fork. We demonstrated that NCOA4 couples the control of DNA replication activation to intracellular iron levels. Indeed, NCOA4 acts as iron sensing protein which upon low iron conditions increases its binding onto chromatin to block activation of DNA replication origins. Loss of NCOA4 in cells promotes unscheduled entry in S phase, replication stress and DNA damage with decreased cell viability.

In this thesis, we demonstrated that the function of NCOA4 in coupling iron levels to DNA replication is relevant for tissue regeneration. Mice with genetic inactivation of NCOA4 (NCOA4 KO) displayed impaired intestinal regeneration after epithelial injury induced by Sodium Dextran Sulfate compared to WT animals, due to accumulation of DNA damage, activation of apoptosis and reduction of intestinal stem cell pool. Furthermore, we demonstrated that NCOA4 activity also affected the proliferation of bone marrow derived cells. BM-derived cells from NCOA4 KO mice exhibited a significant self-renewal reduction after 5-FU treatment compared to WT ones. Since NCOA4 was involved both in controlling iron availability and DNA replication activation we investigated which of NCOA4 functions mainly affected proliferation. We treated mice with iron dextran injections to supply iron availability to sustain tissue regeneration during DSS treatment. We confirmed that, despite iron supply, NCOA4 KO mice showed reduced intestinal regenerative response and presence of DNA damage after DSS treatment. Additionally, we used HeLa cells stably silenced for NCOA4 to evaluate Fe-S clusters enzymes expression in silenced cells at the steady state and upon iron chelation with Deferoxamine. In this condition, the expression of Fe-S clusters enzymes was not affected by the absence of NCOA4. All together our findings indicated a crucial role for NCOA4 in tissue regeneration and cellular proliferation. Particularly, it is the NCOA4 control of DNA replication origins activation, more than the ferritin degradation, to be essential for an appropriate tissue regeneration.

# 1. INTRODUCTION

## 1.1 The essential role of iron in cellular biology

Iron represents an essential element in biology, functioning as a cofactor for several enzymes involved in multiple cellular processes including oxygen binding and transport, ATP production, DNA biosynthesis and repair (G. Papanikolaou and Pantopoulos 2005) (Puig et al. 2017). Iron biological peculiarity consists in its capacity to act as electron donor and acceptor. Thus, iron can readily convert between two common oxidation states  $\text{Fe}^{2+}$  (ferrous) and  $\text{Fe}^{3+}$  (ferric), by the loss or gain of one electron. Iron chemical reactivity has important implication for its biological properties.  $\text{Fe}^{2+}$  undergoes spontaneous aerobic oxidation to  $\text{Fe}^{3+}$  that is virtually insoluble at physiological pH. Thus, despite its high abundance in food, iron uptake is challenging for organisms. Moreover, free iron catalyses the formation of radical oxygen species (ROS) via the Fenton/Haber-Weiss reaction, damaging cellular macromolecules and causing tissue injury. Consequently, a tight control of iron metabolism is necessary to both satisfy metabolic needs for iron and simultaneously to prevent accumulation of toxic iron excess (George Papanikolaou and Pantopoulos 2017)

## 1.2 Iron uptake

The regulation of body iron content depends mainly on the control of dietary iron absorption since mammalian cells lack a mechanism for controlled iron excretion. The two major forms of dietary iron are non-heme iron and heme iron. The mechanism of non-heme iron absorption is well characterised and occurs into the proximal duodenum. Firstly, the ferric iron ( $\text{Fe}^{3+}$ ) is reduced to ferrous iron ( $\text{Fe}^{2+}$ ) by the Reductase Duodenal Cytochrome b (DCYTB) or other ferrireductase in the duodenal lumen (McKie 2001).  $\text{Fe}^{2+}$  is then transported across the apical membrane of enterocytes via the divalent metal transporter 1 (DMT1) (Canonne-Hergaux et al. 1999). Once absorbed,  $\text{Fe}^{2+}$  can be stored within the cytosolic multiprotein complex ferritin, which represents a sort of nanocage for iron (see later), or can be exported at the basolateral membrane via the transmembrane protein ferroportin 1 (FPN1) in order to enter circulation. The efflux of iron via ferroportin 1 is coupled to the re-oxidation of  $\text{Fe}^{2+}$  to  $\text{Fe}^{3+}$  by the membrane-bound multicopper ferroxidase hephaestin or the soluble ceruloplasmin (Vashchenko and MacGillivray 2013) (Donovan et al. 2000). The pathway for heme iron absorption is not completely characterized, but several evidences suggest the occurrence of receptor-mediated endocytosis in the apical membrane of enterocyte. Then, heme iron assimilation requires heme catabolism by heme oxidase to release  $\text{Fe}^{2+}$ . Once liberated from heme, iron follows the same fate of absorbed non-heme iron.

### 1.3 Iron distribution

After being exported by ferroportin,  $\text{Fe}^{3+}$  is rapidly bound by transferrin, the plasma iron carrier, containing two iron binding sites. The circulating transferrin contains a very small but highly dynamic fraction of body iron that turns over  $>10$  times per day to satisfy the daily iron requirement for several cellular processes, mainly erythropoiesis (Aisen 2004). Diferric transferrin binds to the high-affinity transferrin receptor 1 (TfR1) that is ubiquitously expressed on the surface of cells (Ohgami et al. 2005). After iron-loaded transferrin binding to TfR1, the Tf- $\text{Fe}_2$ /TfR1 complex is internalized and iron  $\text{Fe}^{3+}$  is released within the endosome. Iron is then reduced to  $\text{Fe}^{2+}$  by STEAP3 and transported into the cytosol by DMT1 (Muckenthaler et al. 2017). Finally, the Apo-Tf/TfR1 complex returns to the cell membrane, where Apo-Tf dissociates and is available to recapture iron (Fig. 1.1). The newly acquired iron, following the DMT1-mediated transport across the endosomal membrane to the cytosol becomes part of the *labile iron pool* (LIP). (Kakhlon and Cabantchik 2002). This is a transient pool of redox-active iron, presumably associated with several low molecular-weight chelates. LIP represents only a minor fraction of total cellular iron (3-5%), but it reflects the cellular iron status (Kruszewski 2003)

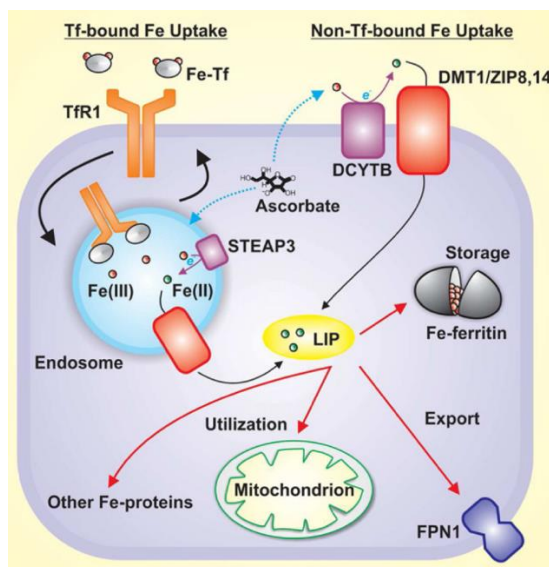


**Figure 1.1 Iron distribution**

Under physiological conditions, most Fe is bound to Tf which binds to the transferrin receptor 1 (TfR1) on the cell surface that is then involved in receptor-mediated endocytosis with the Fe being released from Tf by a decrease in endosomal pH and reduction by an endosomal reductase [e.g., six transmembrane epithelial antigen of the prostate 3 (STEAP3)]. The  $\text{Fe}^{2+}$  is then transported across the endosomal membrane by divalent metal transporter 1 (DMT1) where it then becomes part of the poorly characterized labile iron pool (LIP) in the cytosol. Iron of LIP acts as an intermediate and can be utilized for storage in the iron storage protein, ferritin, or used for synthesis of heme and iron-sulfur clusters in the mitochondrion or cytosol. Iron can also be exported from the cell by ferroportin 1 (FPN1) (modified from Lane et al. 2015)

Cytosolic iron can enter the mitochondria via the SLC transporter mitoferrin (Mfrn) that is localized to the inner mitochondrial membrane (Shaw et al. 2006). Once inside the mitochondria, iron is utilized for the biosynthesis of heme or iron-sulfur clusters, which are pathway of paramount importance for cellular metabolism (Lill 2009) (**Fig. 1.1**). Iron that is not immediately required for metabolic purposes can be exported or stored.

Cells exports iron in its  $\text{Fe}^{2+}$  state via ferroportin 1. To be efficiently exported iron requires extracellular oxidation. This reaction is accomplished by the ferroxidase hephaestin (HEPH) ubiquitously expressed and by ceruloplasmin (CP) specifically expressed by macrophages (**Fig. 1.1**). Iron from the labile iron pool that is not utilized or exported is stored within a cytosolic heteropolymer also known as ferritin. This protein is made of 24 subunits of heavy (FTH1) and light (FTL) chains. FTH1 and FTL are ubiquitous but their expression varies between tissues and in response to physiological conditions. FTH1 displays ferroxidase activity required for iron mineralization into the ferritin nanocage, each of which can accommodate up to 4,500 iron atoms, while the enzymatically inactive light chain promotes the transfer of electrons across the protein shell of the polymer. Iron stored within ferritin is in a non-toxic form (redox-inert) and contributes to intracellular iron bioavailability because it can be mobilized following ferritin degradation by lysosomes (Arosio, Ingrassia, and Cavadini 2009) (**Fig. 1.1**).

#### **1.4 Regulation of iron homeostasis**

Cellular iron uptake, utilization, storage, and transport are coordinately controlled by post-transcriptional mechanisms involving the iron responsive element (IRE)/ iron regulatory protein (IRP) system. Several proteins involved in iron metabolism are encoded by mRNAs containing one or more IREs in their 5' or 3' untranslated regions (UTRs). IRPs consist of two proteins: IRP1 and IRP2 which are activated upon iron deficiency condition and function as inhibitors or promoters of proteins that regulate iron metabolism (Pantopoulos 2004). Either of the two IRPs inhibits translation initiation when bound to the IRE located in the 5' UTR of the mRNAs encoding FTH1, FTL, FPN, ALAS2 (erythroid-specific 5-aminolevulinic acid synthetase 2, a key enzyme for heme biosynthesis) and HIF-2 $\alpha$ . Conversely, IRPs binding to IREs within the 3' UTR stabilizes TfR1 and DMT1 mRNAs. Under conditions of iron deficiency, these processes allow increased iron uptake and transport via respectively TfR1 and DMT1 and prevent storage into ferritin and efflux via ferroportin. On the contrary, an increase in iron supply prevents IRPs from binding to IREs and allows an opposite response. Thus, IRP binding to IREs is regulated primarily by cellular iron availability, although the IRPs do not sense iron fluctuation directly. Upon normal iron conditions, IRP2 interacts with FBXL5 (F-Box and Leucine-Rich Repeat Protein 5) which recruits an E3 ligase complex promoting IRP2 ubiquitination and proteasomal degradation. FBXL5 has an iron sensing

site by which depends the accumulation or degradation of IRP2. On the other hand, IRP1 is regulated by a Fe-S cluster switch. Upon normoferric condition the binding of the Fe-S cluster confers aconitase activity to IRP1 and precludes IRE binding, while in low iron condition IRP1 loses its Fe-S cluster and enzymatic activity and adopts its IRE-binding conformation (George Papanikolaou and Pantopoulos 2017).

An accurate regulation of iron absorption is crucial to prevent systemic iron excess or deficiency. At systemic level the regulation is mainly accomplished via the hepcidin/ferroportin axis. Hepcidin is synthesized in hepatocytes as a pre-peptide that undergoes proteolytic processing to a mature peptide consisting of 25 amino acids. The role of this peptide is to restrict iron fluxes to the bloodstream. Thus, ferroportin (FPN1) is the only known transporter that is responsible for the efflux of iron from cells and hepcidin acts by binding to ferroportin 1 on target cells, mostly macrophages and enterocytes (but also other cell types), triggering phosphorylation, internalization and degradation of ferroportin 1 (Nemeth 2004). Downregulation of ferroportin 1 by hepcidin in splenic and hepatic macrophages decreases the ability of macrophages to export recycled iron from senescent red blood cells (RBCs), which constitute the primary source of iron in the plasma. In addition, a high concentration of hepcidin in the blood blocks the transport of iron out from intestinal epithelial cells, further limiting iron uptake.

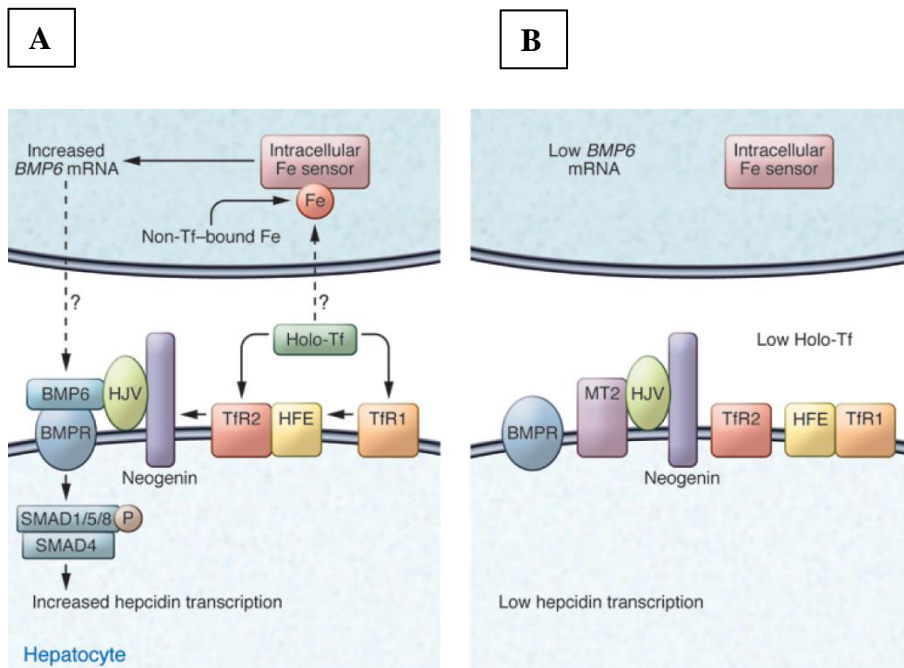


**Figure 1.2 Iron regulation of hepcidin expression.**

**A** Under high iron conditions, increased loading of Tf with iron stabilizes Tfr2, disrupts the HFE-Tfr1 interaction, and induces BMP6 secretion from the nonparenchymal cells of the liver, which facilitates the formation of a complex consisting of the BMP receptor/BMP6/HJV/neogenin/Tfr2/HFE to induce hepcidin expression. **B** Low iron conditions increase MT2, which induces the cleavage of hepatic HJV. Decreased Tf saturation in the circulation destabilizes Tfr2 protein and facilitates the HFE-Tfr1 interaction. Low iron levels in the liver reduce BMP6 secretion from the nonparenchymal cells, consequently blunting BMP signaling and lowering hepcidin expression. (modified from Zhao, Zhang, and Enns 2013)

The expression of hepcidin is transcriptionally regulated by several factors, such as: iron availability, inflammation, and erythropoiesis. Increased serum or tissue iron triggers transcriptional induction of hepcidin in hepatocytes (**Fig 1.2**).

It is well established that iron signals from hepatic iron stores are transmitted to the hepcidin promoter via bone-morphogenetic proteins (BMPs) and SMADs pathway. The activation of the BMP signaling starts with hemojuvenile (HJV) that binds to BMP ligands (BMP2-6) on the cell membrane promoting their interaction with type II BMP receptors (ACVR2A and BMPR2) (Babitt et al. 2006; Healey et al. 2015). Then, HJV is released allowing the interaction of the complex (BMP ligand-BMP receptor type II) with the endosomal type I BMP receptors (ALK2 and ALK3) in order to initiate the signal transduction consisting in the phosphorylation of SMAD1, SMAD5 and SMAD8 proteins, followed by their interaction with SMAD4 and the translocation of the complex to the nucleus. Once into the nucleus the formed complex binds to the two BMP responsive elements (BMP-RE1 and BMP-RE2) at proximal and distal sites of the hepcidin gene (*HAMP*) promoter. Even though various BMPs were found to

induce hepcidin expression, the iron-regulated BMP6 appears to be the major physiologically relevant ligand. BMP6 is secreted from liver endothelial cells in response to increased hepatic iron stores and acts in a paracrine way on hepatocytes. BMP6 was also demonstrated to promote termination of iron signalling to hepcidin by a negative feedback mechanism involving induction of matriptase-2 expression, a serine protease that cleaves and inactivates HJV (Meynard et al 2011; Silvestri et al. 2008). Recent works have demonstrated that also plasma iron (circulating iron) levels regulates hepcidin expression. The mechanism by which extracellular iron levels activate the BMP pathway is still controversial, but some molecules are identified as strong candidate in these last years. Tfr2 is considered the best candidate for sensing extracellular holotransferrin. Tfr2 has a minor affinity for transferrin respect to the Tfr1 but is stabilized by holotransferrin. Another candidate of circulating iron sensing pathway is the hemochromatosis-related membrane proteins HFE. Holotransferrin and HFE are found to compete for binding to Tfr1. HFE and Tfr2 regulate hepcidin expression by their interaction with HJV. Under conditions of high saturation of transferrin, Tfr1 is completely recognized by holotransferrin, resulting in a decreased HFE-Tfr1 interaction, with a consequent increased Tfr2 stability and association with HFE and HJV. The complex facilitates HJV-induced hepcidin expression. On the contrary during iron deficiency, transferrin saturation decreases and Tfr1 can sequester HFE to prevent its binding to Tfr2. The result is a reduced interaction between HFE, Tfr2 and HJV, leading to a downregulation of hepcidin expression (Zhao, Zhang, and Enns 2013).

Moreover, a membrane serine protease matriptase-2 (also called TMPRSS6) functions as a negative regulator of hepcidin-related BMP signaling. TMPRSS6 is expressed mainly in the liver where it acts on HJV, the only known substrate of TMPRSS6. TMPRSS6 suppresses hepcidin expression by cleaving and inactivating HJV. This process results in decreased hepcidin expression (Du et al. 2008)

Hepcidin expression is also regulated by inflammation by an acute hypoferremic response that is caused by iron retention in macrophages to be protective for the host during infection. Interleuchin-6 (IL-6) was found to activate via JAK1/2-mediated phosphorylation the transcription factor STAT3, which binds to a STAT3-binding site (STAT3-BS) in the proximal HAMP promoter and activates hepcidin transcription. (Verga Falzacappa et al. 2007). IL-6-mediated induction of hepcidin was demonstrated to require the BMP type 1 receptor ALK3 (Wrighting and Andrews 2006). Moreover, also other factors were demonstrated to regulate hepcidin expression such as Il-22 and INF-alpha by inducing hepcidin expression via JAK/STAT pathway.

On the other hand, hepcidin expression is downregulated by erythropoiesis, anaemia and hypoxia. Systemic erythropoiesis is regulated by erythropoietin (EPO) production by the kidney. EPO is a key regulator of erythropoiesis; it binds to EPO receptors on the surface of erythroid progenitors, and via the JAK/STAT5 signalling pathway, it prevents apoptosis and induces their

proliferation and differentiation into RBCs. Moreover, EPO stimulates the production of Erythroferrone (ERFE). ERFE is able to suppress hepcidin production in response to erythropoietic stimuli. The mechanism by which ERFE suppresses hepcidin expression remains to be characterized. (George Papanikolaou and Pantopoulos 2017)

### **1.5 The role of iron in erythropoiesis**

Efficient erythropoiesis requires a fine tuning between erythrocyte production, iron supply and hemoglobin synthesis. This requires a crosstalk between bone marrow and liver. The bone marrow tissue uses more than the 80% of plasma iron to produce high amounts of erythrocytes. As already mentioned, maturation and proliferation of early erythroid progenitors depends mostly on EPO. In cases of acute demands, such as haemorrhage and haemolysis, increased EPO secretion stimulates proliferation of erythroid progenitors, and accelerates terminal erythrocyte maturation.

Iron demand increases during the terminal stages of erythroid cell differentiation where the hemoglobin and heme synthesis occurs. Heme is synthesized by a series of enzymatic reactions that take place in the cytosol and mitochondria. The first step is catalyzed in the cytosol by erythroid aminolevulinic acid synthase (ALAS2). In the final step, iron incorporation into protoporphyrin IX takes place in the mitochondria and is catalyzed by ferrochetalase (FC). The transfer of iron to mitochondria is extremely efficient and involves the transporter mitoferrin 1 in the inner mitochondrial membrane. Iron entry in erythroid precursor is the limited step for erythroid heme synthesis. This is mediated by TfR1, which is indispensable for erythropoiesis. Expression of TfR1 peaks in the late basophilic-polychromatophilic stage of maturation and decreases at the orthochromatic stage. In addition, also others proteins associated with iron sense in the liver are expressed in erythroid cells (George Papanikolaou and Pantopoulos 2017).

### **1.6 The role of iron in cell cycle progression**

To grow and divide, normal cells progress through cell cycle in a regulated manner. The cell cycle consists of five distinct phases: G1, S, G2 and M and the progression depends by several checkpoints G1/S, S, G2/M and M-phase (**Fig 1.3**). The control of cell cycle and checkpoints is attributed mainly to the activity of two classes of proteins: cyclin dependent kinases (Cdks), serine/threonine kinases and their binding protein cyclins. Together cyclins and Cdks form a complex and regulate the different phases of cell cycle.

Indeed, progression through G1 is mediated by the expression of cyclin D/cdk4-6, during the late G1 phases cyclin E/cdk2 ensure the progression to the S-phase,

while S and G<sub>2</sub> progression are characterized by the expression of cyclin A/cdk2 cyclin A/cdk1, respectively. Finally, cells enter in M phase via activation of B/cdk1 (**Fig 1.3**) (Sherr 2000).

During the early G<sub>1</sub> phase Cdk4 and/or Cdk6 are activated by cyclin D and initiate phosphorylation of the retinoblastoma protein (Rb) (Sherr 2004). Accumulation of cyclin D/Cdk4-6 complexes allow the saturation of cip/kip Cdk inhibitors (p27, p21) and the activation of cyclin E-Cdk2 complexes. Such complexes by hyperphosphorylating RB induce the release of E2F transcription factors that, in turn, promote transcription of genes necessary to initiate and sustain DNA replication. Later Cdk2 plays an important role in S phase progression by complexing with cyclin A. Cyclin A is synthesized at the onset of the S phase and phosphorylate proteins involved in DNA replication (Coverley et al. 2000). During the G<sub>2</sub>/M transition, cyclin A/Cdk1 activity is required for the initiation of prophase. Finally, the G<sub>2</sub>/M transition occurs upon peaking of cyclin B/Cdk1 complexes activity. Drop of cyclin B allows M phase completion and exit.

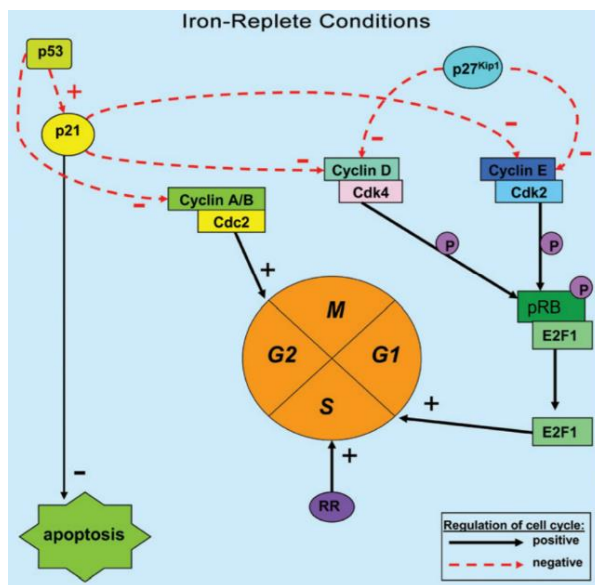


**Figure 1.3 Summary of the cell cycle in normal Fe-replete cells.**

The cell cycle consists of four main phases: G<sub>1</sub>, S, G<sub>2</sub> and M-phase. Under normal conditions in Fe-replete cells, the progression of the cell cycle is controlled by a number of molecules including the cyclins A, B, D and E, as well as the cyclin-dependent kinases (cdks). Cyclin D1 forms a complex with cdk4, while cyclin E binds with cdk2, allowing them to become active enzymes. These complexes are then involved in phosphorylation of the retinoblastoma susceptibility gene product (pRb), which allows the release of the transcription factor, E2F1. Once free, E2F1 can translocate to the nucleus where it mediates the transcription of a range of genes vital for S-phase progression. One of the most important mediators of this G<sub>1</sub>/S checkpoint is p53, which can cause G<sub>1</sub>/S arrest under conditions of cell stress or DNA damage. One function of p53 is to transactivate the expression of the cdk inhibitor, p21CIP1/WAF1, which then inhibits the activity of cyclin D1/cdk4- and cyclin E/cdk2 complexes, thereby preventing entry into S-phase. In addition, p53 is also able to inhibit cyclins A and B leading to G<sub>2</sub>/M arrest. (Modified from Yu, Kovacevic, and Richardson 2007)

The regulation of cyclin-cdks activity is accomplished by cdk inhibitors (CKI). CKIs are divided in kinase inhibitor proteins (CIP/KIP) and inhibitors of cdk4/6 (INK4) (Vidal and Koff 2000).

The CIP/KIP family of inhibitors consists of several proteins, such as p21, and p27 which by directly binding cyclin/cdk complex inhibits their activity, except for cyclin D/cdk4-6. Thus, p21 and p27 are required for the assembly, nuclear accumulation, and stabilization of the cyclin D/cdk4-6 complexes particularly during mid-G1 phase of cell cycle. In contrast, the inhibitory activities of INK4 are restricted to cdk4-6. As a consequence, the INK4 family is thought to play a major role in regulation of G1/S checkpoint (Le 2002).

Another important regulator of cell cycle is p53, also known as tumor suppressor protein. p53 is a critical transcription factor that is activated upon stress condition. Once activated, p53 can initiate the transcription and subsequent expression of various downstream genes that induce differentiation, senescence, DNA repair, cellular arrest/or apoptosis (Castillo et al. 2005). Due to p53 function, its stability, expression and activation is tightly regulated by the murin double minute-2 (mdm2) protein, that acts as a ubiquitin ligase to mediate p53 degradation (Carr 2000).

There are many stress events that can affect the regulation and consequently the progression of cell cycle such as DNA damage, decreased dNTPs levels, hypoxia, loss of survival signals and abnormal cell growth.

More recently new evidence supported the role of intracellular iron levels to additionally control cell cycle progression. Depletion of iron with chelators such as deferoxamine (DFO) has been demonstrated to affect various cell cycle proteins and molecules inducing cell cycle arrest.

As described before, cyclins and Cdks are key regulators for the normal progression through the cell cycle. Iron depletion mediated by chelators affects the expression of several cyclins and cdks. In fact, under low iron conditions cyclin D1 levels decreases (Alcantara 2001). Considering the rate-limiting role that cyclin D1 plays in G1/S progression, its regulation by iron appears to be important to prevent entrance into the S phase, when iron is essential for RNR activity and thus DNA synthesis (see later). Also, cdk2 levels are reduced during iron depletion, preventing E2F release by RB. The release of E2F1 is necessary to transcribe genes essential for cell cycle progression, such as cyclin A and cyclin E. The molecular pathways that in low iron promote reduction of cyclins D, E and A and of cdk2 are not known in details (Le 2002).

Intracellular iron levels also affect numerous proteins involved in DNA replication and repair that require iron as cofactor. These proteins include the three DNA polymerases (Pol $\alpha$ , Pol $\delta$  and Pol $\epsilon$ ), the DNA helicases (Rad3/XPD, FancJ) and DNA primase regulator subunit PRIM2. All these proteins contain a conserved Fe-S cluster in their structure that ensure the correct function and consequent regulation of DNA replication (Netz et al. 2012). Thus, iron depletion causes a reduced production of such enzymes with consequent lag or even arrest of DNA replication (C. Zhang 2014).

The Ribonucleotide Reductase (RNR) is an enzyme that catalyzes the biosynthesis of deoxyribonucleotides essential for DNA replication, cell cycle progression and DNA repair. This process requires a tyrosyl free radical which acts to reduce the corresponding ribonucleotides to deoxyribonucleotides. Human RNR consists of two non-identical homodimers, R1 and either R2. The R1 protein contains the active sites and binding sites for allosteric effectors, while the R2 subunit contains one di-nuclear Fe center and one stable tyrosyl radical, vital for the enzymatic activity (Y. Zhang et al. 2008). Since the reduction of ribonucleotides is the rate-limiting step of DNA synthesis, inactivation of RNR has several consequences, such as inhibition of DNA synthesis, cell proliferation and DNA repair, leading to cell cycle arrest and apoptosis. As iron is required for the enzymatic activity of RNR, iron depletion is well known to effectively inhibit the activity of this enzyme (Kumar et al. 2010).

Finally, also the Hypoxia inducible factor-1 (HIF-1) is influenced by intracellular iron levels. Upon low iron levels HIF-1 accumulates in the cell, and translocates to the nucleus where it binds to HIF-1 $\beta$  to form the HIF-1 complex to regulate several genes by binding to their hypoxia-responsive element (HRE). For example, TfR1 is transcriptionally upregulated by HIF-1 to increase intracellular iron levels. HIF-1 activation results not only in increasing iron levels, but also in cell cycle arrest, apoptosis, and inhibition of growth.

All these evidences demonstrate that appropriate iron availability is a critical determinant for cell cycle progression. Cellular iron depletion results in G1/S arrest and, if severe and prolonged, apoptosis. Thus, the coordinated activity in response to iron level of a number of proteins such as RNR, DNA synthesis and repair enzymes, HIF-1, cyclins and cdks provide a strict control on cell cycle progression (Yu, Kovacevic, and Richardson 2007).

### **1.7 The Nuclear Receptor Co-Activator 4**

The Nuclear Receptor Co-Activator 4, also known as NCOA4, is a 70 kDa protein composed by 614 amino acids divided in an N-terminal and C-terminal portion. The N-terminal portion includes two nuclear receptor binding motifs the LXXLL (a.a 92-96) and FXXLF (a.a 328-332) motifs which enable NCOA4 to bind several nuclear receptors. The FXXLF motif enables the interaction of NCOA4 with the androgen receptor (AR) thus NCOA4 was also referred as AR-associated protein 70 (ARA70) (Yeh e Chang 1996). Then, subsequent studies revealed LXXLL nuclear motif essential for the interaction of NCOA4 with estrogen (ER), progesterone (PR), glucocorticoid (GR), Vitamin D (VDR), thyroid hormone (TR) and peroxisome proliferator-activated  $\alpha$  and  $\gamma$  (PPAR $\alpha/\gamma$ ) receptors (Kollara and Brown 2012). Moreover, the N-terminal portion also presents a coiled-coiled domain (aa 17-125), a structural motif in which alpha-helices are coiled together allowing NCOA4 oligomerization. The coiled-coil

domain of NCOA4 is a part of the RET/PTC3 oncogenic fusion protein found in papillary thyroid carcinomas (PTCs). The RET/PTC3 chromosomal rearrangement results from the fusion of the sequences encoding the tyrosine kinase domain of the receptor tyrosine kinase RET with the sequences encoding the first 238 aa of NCOA4. This fusion protein leads to the ligand-independent dimerization of RET/PTC protein, resulting in chronic stimulation of MAPK and PI3K-AKT signalling and increased cell proliferation and transformation in thyroid cells (Santoro et al. 1994). The N-terminal portion of NCOA4 also presents a binding site to MCM7, a component of the DNA helicase. Our group have demonstrated that NCOA4 directly interact with the MCM7 and induces the block of DNA replication origin activation during S phase (Bellelli et al. 2014).

Recently NCOA4 was found to be involved in regulation of iron metabolism in a new process known as “Ferritinophagy”. Through its C-terminal portion NCOA4 interacts with ferritin, the intracellular iron storage protein and promotes ferritin lysosomal degradation with consequent release of iron. Specifically, two amino acid residues have been identified essential for NCOA4 binding to ferritin: Tryptophan 497 (W 497) and Isoleucine 498 (I 498), both interacting with the conserved surface Arginine 23 (R 23) of ferritin heavy chain (FTH1) (Mancias et al. 2014).

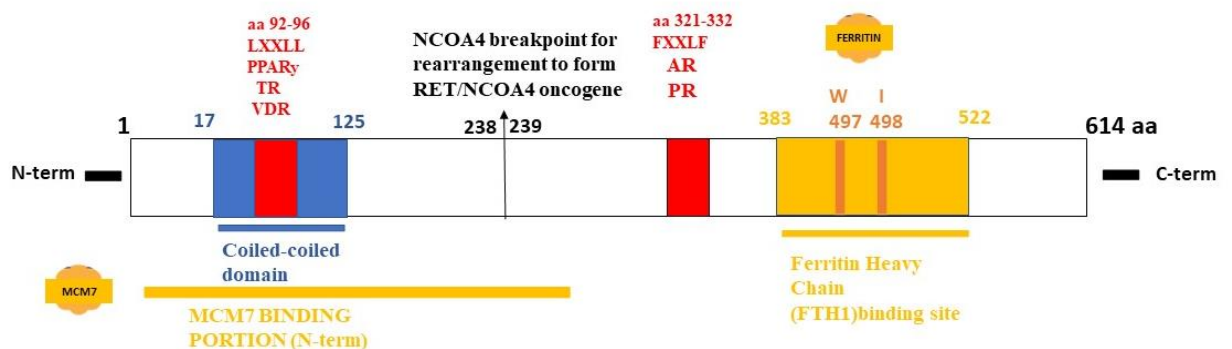


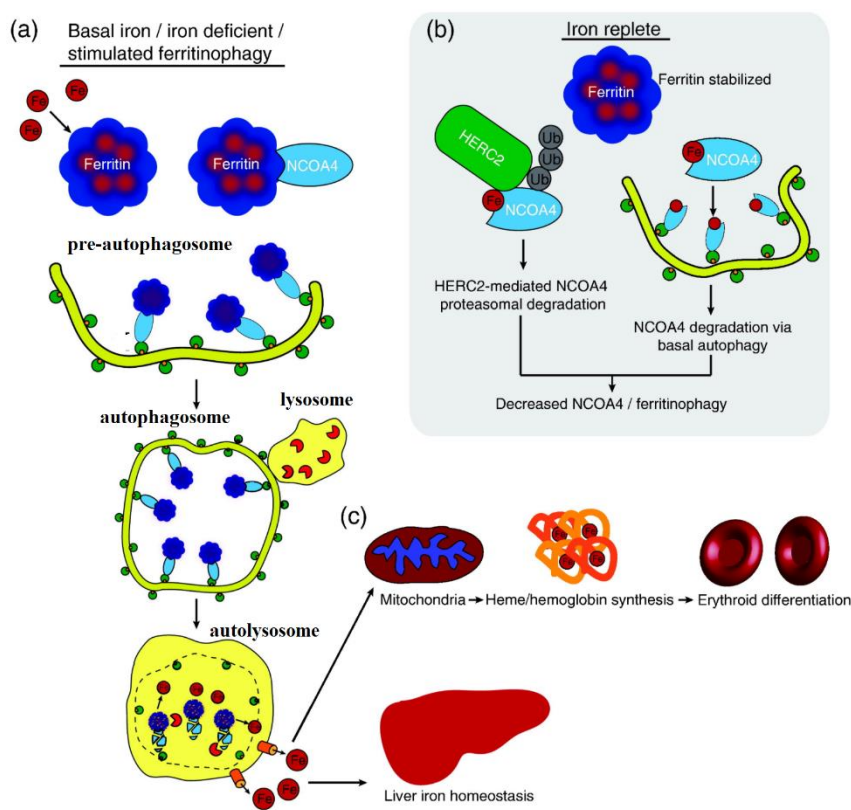
**Figure 1.3 NCOA4 protein structure**

The protein is codified by 614 aa. The N-terminal portion presents a coiled coiled domain (aa 17-125), the MCM7 binding site and the nuclear receptor binding domain LXXLL (aa 92-96). The C-terminal portion presents the site for Ferritin heavy chain (FTH1) interaction (aa 383-522) and the nuclear receptor binding domain FXXLF (aa 321-332)

## 1.8 NCOA4 regulates Ferritinophagy

Ferritin has been usually described as an iron storage protein which implies a static role for this protein, but recent evidence demonstrates a dynamic and active

role of ferritin in regulating iron availability. Ferritin was demonstrated to undergo lysosomal degradation in order to actively sustain release and recycling of iron (Arosio, Elia, and Poli 2017). This cellular process is called Ferritinophagy and is sustained by the Nuclear Receptor Co-Activator 4 (NCOA4). NCOA4 acts as a cargo receptor by binding ferritin and delivering it to the lysosomes. Once into the lysosomes, ferritin is degraded and allows the release of stored iron (Mancias et al. 2014). This process occurs continuously at basal levels under conditions of iron balance and is upregulated when cells suffer from iron deficiency.



**NCOA4-mediated ferritinophagy pathway.** a) Iron (Fe) is sequestered by ferritin complexes containing ferritin heavy and light chains. NCOA4 recognizes ferritin and delivers it to an incipient autophagosome. Degradation of ferritin in autolysosome allows iron release and export to the cytosol. (b) NCOA4 levels and thereby ferritinophagy are regulated by iron levels in the cell. Under high iron/iron replete conditions, NCOA4 is recognized by HERC2, and targeted for proteasomal degradation. In tandem, NCOA4 is also targeted for autophagic degradation. A lower level of NCOA4 therefore decreases flux through the ferritinophagy pathway. (c) Liberated iron can be used in many iron-dependent processes including heme synthesis, which is required for hemoglobin synthesis during erythroid differentiation and for maintenance of liver iron homeostasis (modified from Mancias e Kimmelman 2016)

Give the essential role of NCOA4 in controlling ferritin degradation, it is not surprisingly that NCOA4 intracellular levels are themselves controlled by iron

status. Indeed, in iron replete condition NCOA4 abundance is low, thereby promoting ferritin accumulation. On the contrary in low iron NCOA4 levels increase, promoting ferritinophagy. The levels of NCOA4 are controlled by an E3-ubiquitin ligase also known as HERC2. In iron replete condition, HERC2 recognized iron-bound NCOA4 and promotes its polyubiquitination and proteasomal degradation.

The role of NCOA4 in controlling ferritin degradation could be considered as a second layer of regulation in cytosolic iron homeostasis after the iron dependent binding of IRPs to IREs for the coordinated regulation of ferritin and other regulatory proteins of iron metabolism. The importance of NCOA4 in iron regulation was also confirmed using NCOA4-deficient (NCOA4 KO) mice that showed iron accumulation in the liver and spleen, increased levels of transferrin saturation, serum ferritin, and liver hepcidin, and decreased levels of duodenal ferroportin (Bellelli et al. 2016). An iron-enriched diet caused NCOA4 KO mice premature death with liver damage, while on an iron-deprived diet NCOA4 KO mice developed severe microcytic hypochromic anaemia and ineffective erythropoiesis associated with increased erythropoietin levels. This mouse model confirmed that NCOA4 prevents ferritin and tissue iron accumulation and is required to sustain erythropoiesis in low iron conditions (Bellelli et al. 2016). Moreover, ferritinophagy was also demonstrated to occur during terminal erythroid differentiation (Mancias et al. 2015) and coincides with NCOA4 expression in orthochromatic erythroblasts (An et al. 2014).

### **1.9 NCOA4 blocks DNA replication origins activation**

DNA replication is a finely regulated process. Eukaryotic cells have developed mechanisms to ensure fidelity of DNA replication and to preserve genome stability. DNA replication starts at specific genomic regions defined as DNA replication origins. The activation of the DNA replication origins encompasses principally two events: the loading of the pre-RC complex, a reaction also known as replication origin “licensing” and the activation of origins which is referred as “firing” (Fragkos et al. 2015).

The origin licensing reaction takes place at all the potential replication origins of the genome during G1 phase of the cell cycle, although only a group of them will be activated during the S-phase (Leonard and Mechali 2013). The process of origins licensing is divided in several steps during the G1 phase. Firstly, the origin recognition complex (ORC1-6) is recruited to replication origins and followed by the binding of CDC6 and CDC10-dependent transcript (CDCT1) onto DNA origins (Bowers et al. 2004). This event allows the recruitment of the mini-chromosome maintenance (MCM) complex. The MCM complex is a hexamer composed by 6 subunits MCM2-7. A double hexamer of MCM2-7 is recruited onto the DNA and represents the core of the DNA helicase but in an inactive form. These steps establish the formation of the pre-replication complex (Pre-RC) (Masai et al. 2010).

During the G1-S transition, the Pre-RC is converted into the Pre-IC (pre-Initiation Complex) by the recruitment of new factors. The assembly of Pre-IC is accomplished by a series of phosphorylation events that involve mainly DBF4-dependent kinase (DDK) and cyclin-dependent kinase (CDKs), which are Ser/Thr protein kinases. The binding of DDK and CDKs onto chromatin leads to the direct phosphorylation of several subunit of the MCM2-7 complex. This phosphorylation is an essential step for the subsequent recruitment and formation of the CMG complex, which consists of CDC45, MCM complex and GINS proteins and for the activation of the DNA helicase complex (Heller et al. 2011). The activation of the helicase complex represents the DNA origin firing reaction coinciding with the opening of the replication bubble and the recruitment of other essential proteins such as the proliferating cell nuclear antigen (PCNA), replication protein A (RPA) and DNA polymerases. Finally, these reactions lead to the dissociation of the DNA helicase complex into two functional replication forks that move in opposite directions from each activated origin resulting in the initiation of DNA replication (Fragkos et al. 2015).

Recently, our group found that NCOA4 was involved in regulating the DNA replication origin activation (Bellelli et al, 2014). By a yeast two-hybrid screening, NCOA4 was found to interact with MCM7, a member of the MCM2-7 complex. Notably, NCOA4, via its N-terminal portion directly bound to MCM7 protein in the context of the CMG complex and inhibited the activation of the DNA helicase by preventing the unwinding of DNA and the firing of DNA replication origins.

This function of NCOA4 represents a novel mechanism to negatively control the activation of DNA replication origins. Indeed, in mouse embryonic fibroblasts derived from NCOA4 null mice, the absence of NCOA4 lead to an uncontrolled DNA replication origins activation, with replication stress, activation of DNA damage response and premature cellular senescence (Bellelli et al. 2014, 4)

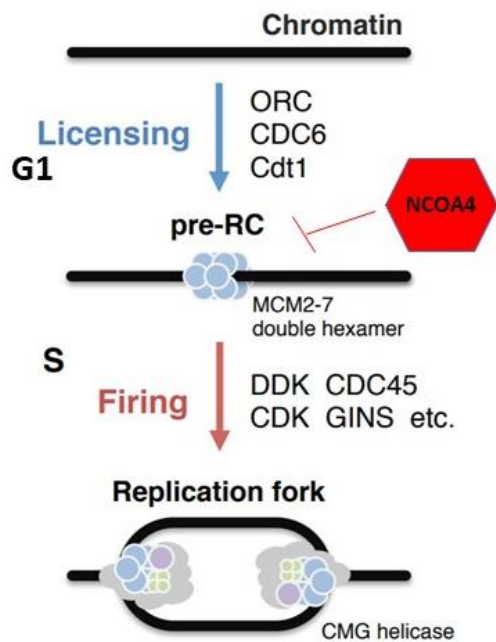


**Figure 1.3. Origin licensing.**

The concerted action of ORC, CDC6, and CDT1 load hexamers of MCM2-7 onto DNA during G1 phase. MCM2-7 double hexamer licenses origins. The Nuclear Receptor Coactivator4 binds MCM7 protein and blocks the activation of DNA origins (modified from Higa, Fujita, and Yoshida 2017)

### 1.10 NCOA4 acts as DNA replication regulator upon iron deprivation

As mentioned before, a correct concentration of intracellular iron levels is required to ensure correct functioning of enzymes involved in DNA metabolism and repair. Indeed, low iron levels not only influence the assembly and consequent activity of DNA polymerases and enzymes involved in DNA repair but also the activity of Ribonucleotide Reductase which provides dNTPs production.

As already discussed, low iron levels affect cell cycle progression. Thus, iron restriction induces a G1/S phase arrest to prevent an inappropriate S phase entry. Since NCOA4 regulates both iron availability via ferritin degradation and DNA replication via MCM7 binding, we asked whether these 2 functions could be related to modulate DNA synthesis versus intracellular iron levels. Our preliminary data revealed that NCOA4 is able to couple iron levels to DNA replication (Federico et al, submitted). Experiments with deferoxamine (DFO), an iron chelator, demonstrated that upon iron deprivation NCOA4 increases its cytosolic levels thereby inducing ferritin degradation and consequent iron release. Additionally, NCOA4 also incremented its nuclear levels thereby interacting with DNA helicase (MCM2-7 complex) and restricting activation of DNA replication origins (Federico et al, submitted). Accordingly, we found that

the absence of NCOA4 in cells causes unscheduled origins firing that results in replication stress and genome instability. Indeed, cells silenced for NCOA4 showed reduced replication fork rate and inter-origin distance and elevated fork asymmetry, indicative of fork stalling. As a consequence of replication stress and fork stalling, the absence of NCOA4 in cells activated ATR/Chk1 DNA damage pathway (Federico et al, submitted).

We also demonstrated that the mutant NCOA4 489-497, unable to bind ferritin and induce Ferritinophagy, was able to interact with MCM7 protein to avoid replication stress observed upon NCOA4 absence in low iron condition. Thus, we found that NCOA4 control of DNA origins activation is essential to ensure correct proliferation (Federico et al, submitted).

## 2. AIM OF THE STUDY

The Nuclear Receptor Coactivator 4 (NCOA4) has been described as a negative regulator of DNA replication. NCOA4 directly interacts with the minichromosome maintenance 7 (MCM7) protein, a key component of the eukaryotic DNA helicase (MCM2-7 complex), to prevent the activation of DNA replication origins (Bellelli et al. 2014). Moreover, it has been demonstrated that NCOA4 is also involved in regulating iron availability. Thus, NCOA4 acts as a cargo receptor for ferritin, the iron storage protein, and promotes its lysosomal degradation and consequent iron release (Mancias et al. 2014).

Iron is an essential microelement for the progression and regulation of cell cycle and represents a cofactor for several enzymes involved in DNA metabolism and repair. As a matter of fact, cells upon iron deficiency exhibited a cell cycle arrest at G1/S phase of cell cycle. Our previous results in HeLa cells, demonstrated that iron deprivation increased NCOA4 binding to MCM7 protein to avoid inappropriate activation of DNA replication origins. Moreover, we found that the absence of NCOA4 in HeLa cells, promoted unscheduled entry in S phase, replication stress and DNA damage with reduced cells viability (Federico et al, submitted).

Hence based on our preliminary data, the aim of this study was to better investigate the relevance of NCOA4 in coupling DNA replication and intracellular iron levels *in vivo* by using C57BL6 mice with genetic inactivation of NCOA4.

To this aim we investigated the relevance of NCOA4 functions in controlling regeneration of high proliferative tissue.

- Firstly, we focus our attention on intestinal tissue. We induced an injury with Sodium Dextran Sulfate (DSS) to stimulate proliferation of intestinal stem cells and consequently we evaluated the regenerative activity of both NCOA4 KO and WT mice.
- Next, we analysed the regenerative response of bone marrow. Upon serial bleeding, we induced a bone marrow proliferative stimulus in mice and then we evaluated *ex vivo* the colony forming ability of BM-derived cells from NCOA4 KO and WT mice.
- Then, we evaluated the self-renewal of BM-derived cells after causing an injury in bone marrow using the 5-Fluorouracil treatment genotoxic agent

The second aim of this study was to distinguish which of NCOA4 functions (control of DNA replication and ferritin degradation) contributed to a correct tissue regeneration.

- To this aim we decided to analyse the intestinal regeneration after injection of iron dextran to supply iron availability thereby sustaining intestinal stem cells proliferation after DSS treatment.
- We evaluated whether the intracellular levels of several Fe-S cluster enzymes after iron deprivation could be affected by the absence of NCOA4 in HeLa cells.

## **3. MATERIALS AND METHODS**

### **3.1 Cell culture**

HeLa cells (ATCC® CCL-2™) were maintained in RPMI medium supplemented with 10% Fetal Bovine Serum (FBS), 50 mg/ml Penicillin-Streptomycin and 2 mM L-glutamine at 37 °C in a humidified atmosphere containing 5% CO<sub>2</sub>.

Hela cells were treated with the iron chelator Deferoxamine mesylate salt (DFO, Sigma-Aldrich, cat. n. D9533) 100 mM. After 2 or 24 hours cells were collected and subjected to total protein extraction as described in 3.4.

### **3.2 Generation of stable clones silenced for NCOA4 protein**

Hela cells were transfected with shRNA control and shNCOA4 plasmids by using the nonliposomal transfection reagent FuGENE® HD (Promega).

After 48h, puromycin was added (2,5 ug/mL) to select cells stably expressing plasmids. After 1 week, clones were picked, plated in 60-mm culture dishes and controlled for NCOA4 protein levels by WB analysis.

### **3.3 Labile Iron Pool (LIP) evaluation**

We evaluated Intracellular iron concentration by using Calcein assay.

Calcein acetoxymethyl ester (Calcein-AM; Sigma-Aldrich; cat. n. 56496) is a membrane permeable reagent which once entered in cells undergoes hydrolysis by esterases to calcein (Ca) and becomes fluorescent. Calcein fluorescence is quenched by iron binding. Thus, the difference in mean fluorescence between DFO-treated and untreated cells was used to calculate the amount of Labile Iron Pool (LIP).

Briefly,  $2,5 \times 10^5$  cells were treated for 30' with 250µM Calcein acetoxymethyl ester). Then, cells were washed with 1X PBS (Phosphate Buffered Saline) and left untreated or incubated with 1 mM DFO-conditioned medium for 1 h. Fluorescence of samples were analyzed by flow cytometer (BD Accuri™ C6). Finally, the difference in the mean fluorescence of DFO-treated and untreated cells was used as a measur of LIP.

### **3.4 Protein extraction**

For protein extraction HeLa cells were washed in 1X PBS and lysed by mechanical scraping in lysing buffer containing 50 mM N-2-hydroxyethylpiperazine-N'-2-ethanesulfonic acid (pH 7.5), 1% (vol/vol) of the

non ionic detergent Triton X-100, 150 mM NaCl and 5 mM EGTA. To inactivate endogenous phosphatases and proteases 50 mM sodium fluoride, 20 mM sodium pyrophosphate, 1 mM sodium vanadate, 2 mM phenylmethylsulphonyl fluoride and 1 ug/ml aprotinin were also added to lysis buffer.

Lysates were clarified by centrifugation at 13,200 rpm for 30 min and supernatants containing proteins extracts were recovered.

Comparable amounts of proteins (50 ug), estimated by Bradford assay (Bio-Rad, Munchen, Germany), were diluted in Laemmli buffer and subjected to SDS-PAGE and direct Western blotting.

Immunoblotting was carried out with specific antibodies: anti-Transferrin Receptor 1 (TfR1) was from Life technologies (Cat.n.136800), anti-Iron Regulatory Protein 2 (IRP2) was from Santa Cruz Biotechnology (sc-33680), anti-Polymerase delta (PolD) (ab168827), | anti-XPB (ab54676), anti-BRP1/FANCD1 (ab49657), anti-Ribonucleotide Reductase 1 (RRM1) (ab133690) and anti-Ribonucleotide Reductase2 (RRM2) (ab57653) was from Abcam.

Secondary antibodies anti mouse or anti rabbit coupled to horseradish peroxidase were from Santa Cruz Biotechnology (Cat. n. 170-5046 and Cat. n. 170-6516)

Immune complexes were detected with the enhanced chemiluminescence kit (Amersham Pharmacia Biotech, Little Chalfort, UK).

### **3.5 Hystology Analysis**

Formalin-fixed, paraffin-embedded (FFPE) sections (6 µm thick) were stained with H&E for 15'' or deparaffinized and rehydrated by passages through xylene and alcohol series (100%,95%,75%,50%) for immunohistochemical (IHC) staining. Then, endogenous peroxidase activity was blocked by treatment with 3% hydrogen peroxide for 10 min at room temperature followed by washes in water. Antigens were retrieved by incubating tissue sections for 15 min at 100° with boiling citrate buffer (citric acid 0.1 M, trisodium citrate 0.1 M, pH 6.0) and then washed with water and 1X PBS.

To block nonspecific binding between primary antibody and tissues, tissues sections were incubated with 1% BSA in 1X PBS for 1h at room temperature followed by 16h incubation with primary antibodies: anti phospho-Histone 3 (Cell signaling technology Cat. n. 5701S), anti-phospho-Checkpoint kinase 2 (Novus Biological Cat. n. NB100-92502), anti-Cleaved caspase3 (Cell signaling technology Cat. n.9661S). Then slides were incubated for 30 min at room temperature with biotinylated goat anti-rabbit antibody (Vector Laboratories, Burlingame, CA, USA); the stain was visualized with 3,3'-Diaminobenzidine (DAB) (SIGMA-Aldrich).

### 3.6 Sodium Dextran Sulfate treatment

- Fifteen 12 months old C57BL6 WT and NCOA4 KO mice were treated with one cycle of 4% Sodium Dextran Sulfate (Sigma Aldrich Cat. n. D8906) dissolved in drinking water. After 7 days, DSS was replaced by normal drinking water and 5 mice were sacrificed. After 3 and 6 days another group of 5 mice were sacrificed.
- To supply iron, fifteen 12 months old C57BL6 WT and NCOA4 KO were subjected to intraperitoneal injections of Iron dextran (1g/kg body weight Sigma Aldrich Cat.n. D8517) before and after one cycle of 7 days 4% DSS treatment. Then mice followed the same experimental plan as previously described.

### 3.7 Rna Extraction and RT-PCR

RNA was isolated from frozen, mechanically fractured colon mice using TRIzol-chloroform extraction method. Briefly, tissues were homogenously resuspended in 1 ml of Trizol reagent (Invitrogen, Carlsbad, CA, USA) and 200 µl of chloroform. Samples were then centrifuged at 13,500 rpm at 4°C for 20 minutes and 500 ul of supernatant was recovered. to precipitate RNA the same amount of isopropanol was added. Next the samples were centrifuged 13,500 rpm at 4° for 20 min. The samples were then washed with 70% ethanol and solubilized in DEPC-water.

1,5 mg of isolated RNA (1.5 mg) was reverse-transcribed by using 50µg/µl M-MLV Reverse transcriptase (Invitrogen™) in a buffer containing 25mM MgCl<sub>2</sub> ), 10 mM dNTPs(Applied Biosystems), 50 mM random examers (Invitrogen) and 20µg/µl RNAsi inhibitor (Applied Biosystems)

Real Time PCR reactions were done in triplicate using SYBR green mastermix (Bio-Rad, Munchen, Germany), and fold changes were calculated with the following formula:  $2^{-\Delta\Delta CT}$ , where  $\Delta Ct$  is the difference between the amplification fluorescence threshold of the mRNA of interest and the mRNA of housekeeping GAPDH gene used as an internal reference.

The primer sequences used for qPCR are:

GAPDH: Forward 5'-3' CATCACTGCCACCCAGAAGACTG  
Reverse 5'-3' ATGCCAGTGAGCTTCCCGTTCAG

Lgr5: Forward 5'-3' CCTACTCGAAGACTTACCCAGT  
Reverse 5'-3' GCATTGGGGTGAATGATAGCA

BMI1: Forward 5'-3' TATAACTGATGATGAGATAATAAGC  
Reverse 5'-3' CTGGAAAGTATTGGGTATGTC

### 3.8 Evaluation of serum Transferrin saturation

Transferrin saturation was calculated as the percentage of the ratio between serum iron and total iron binding capacity (as described in the formula below), using the colorimetric kit of Randox Laboratories (The Total Iron Binding Capacity Kit Ltd.) and following the manufacturer's instructions.

$$\text{TSAT}\% = \frac{\text{Serum iron } (\mu\text{g/dl})}{\text{TIBC } (\mu\text{g/dl})} \times 100$$

### 3.9 5- Fluorouracil treatment

12 months old C57BL6 NCOA4 WT and KO were intraperitoneally injected with 100 mg/ kg body weight of 5-Fluorouracil every 7 days. Mice were sacrificed after 1 or 2 doses of 5-FU and bone marrow-derived cells from femurs were collected.

### 3.10 Colony-forming unit assay

Bone marrow (BM)-derived cells were isolated from femurs of NCOA4 WT and KO mice and recovered in DMEM 10% FBS 50 mg/ml penicillin-streptomycin, and 2 mM L-glutamine. After 2 washes in complete medium, BM-derived cells were counted, and  $2 \times 10^5$  cells were mixed in 5 ml of Methylcellulose (R&D Cat. n. HSC007) and let stand for 20 minutes. Then samples were plated in 35-mm culture dishes and stored at 37°C. After 10 days, BM-derived colonies were counted. To distinguish the formation of erythroid-lineage progenitors-derived colonies (BFU-E, CFU-E) we stained BM-derived colonies with Bendizine which binds heme-group presents in erythroid bone marrow derived cells.

To analyze self-renewal ability of BM-derived cells a serial replating assay were performed. Briefly, after 10 days from the first plating, cells were collected counted and  $2 \times 10^5$  cells were replated with methylcellulose into 35-mm culture dishes. After 10 days from each replate BM-derived colonies from both NCOA4 WT and KO mice were counted.

### 3.11 Survival experiment

12 months old NCOA4 WT and KO mice were used to perform survival analysis.

We conducted survival experiments after two different treatments:

- Six 12 months old NCOA4 WT mice and six 12 months old NCOA4 KO mice were treated with one cycle of 4% Sodium Dextran Sulfate . After 7 days, in both groups of mice DSS was replaced with normal drinking water. We monitored daily body weight as well as the survival of both groups of mice.
- eight 12 months old NCOA4 WT and eight 12 months old NCOA4 KO mice were treated weekly with 1 dose of 5-FU 100 mg/kg body weight. We monitored daily body weight as well as the survival of both groups of mice.

### **3.12 Statistical analysis**

All graphical data illustrations were expressed as means  $\pm$  SEM. Statistical differences were calculated by analysis of t-test Student with Graphpad prism 9.1.0. p-value  $< 0,05$  was referred as \*, p-value  $< 0,005$  was referred as \*\*, p-value  $< 0,0005$  was referred as \*\*\*

## 4. RESULTS

### 4.1 Genetic inactivation of NCOA4 impairs colon regeneration in mice

We wanted to evaluate the relevance of NCOA4 function in coordinating iron availability and DNA replication *in vivo*. Our preliminary data in HeLa cells demonstrated that in low iron the absence of NCOA4 caused impaired cell proliferation due to accumulation of DNA damage (Federico et al, submitted). Thereby, we decided to assess the regenerative capacity of intestinal mucosa upon tissue damage in C57BL6 mice bearing genetic inactivation of NCOA4 (NCOA4 KO) compared to WT animals.

To this aim, we treated both NCOA4 KO and WT mice with Sodium Dextrane Sulfate (DSS) to induce intestinal injury. DSS is a polysaccharide that causes epithelial damage and inflammatory response, resulting in colitis and destruction of intestinal mucosa. WT and NCOA4 KO mice were treated for 7 days with 4% DSS dissolved in drinking water. Intestinal cell proliferation and tissue regeneration was evaluated after 3 and 6 days of release from treatment, as showed in the **Figure 4.1**.

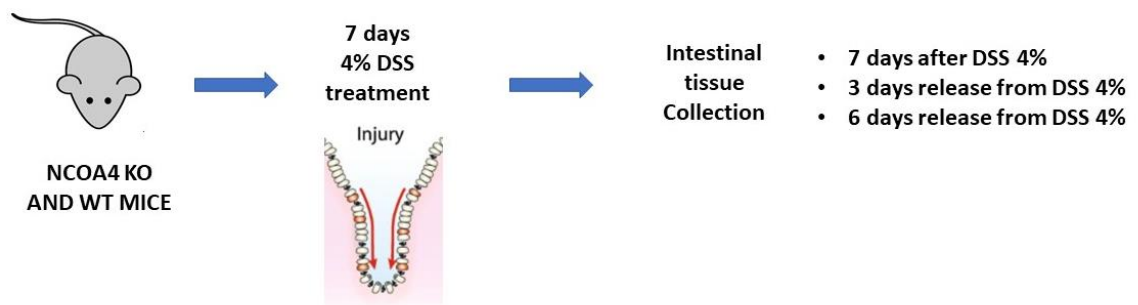


**Figure 4.1 Representative scheme of 4% DSS treatment in NCOA4 KO and WT mice.**

Mice were treated for 7 days dissolving DSS in drinking water (4%). Intestines were collected after 7 days of DSS treatment, and after 3 and 6 days of release from the treatment to analyse the regenerative response of both NCOA4 KO and WT mice.

First, we measured colon length after 0, 3 and 6 days of release from treatment and found that after 7 days of 4% DSS treatment both WT and NCOA4 KO mice displayed a reduced colon length compared to not treated mice (**Fig. 4.2**). Conversely, while WT mice started to increase the colon length after 3 and 6 days of release from the treatment, NCOA4 KO mice were unable to recover colon length (**Fig. 4.2**).

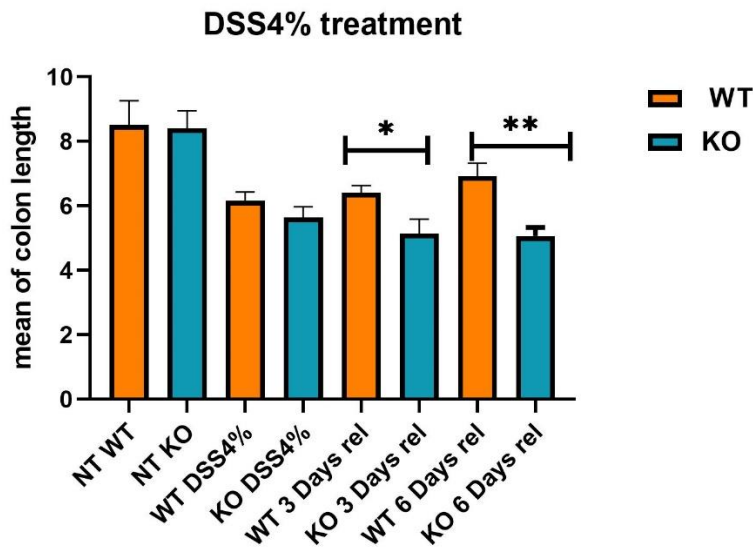


**Figure 4.2** *NCOA4* KO mice exhibited reduced colon length after DSS 4% treatment. *NCOA4* KO and WT colons were harvested, washed, and measured. The graph represented the colon length average for each group of mice WT and *NCOA4* KO after 7 days of DSS and after 3 and 6 days of release from treatment. The values were represented as Mean  $\pm$  SEM  $p$ -value < 0.05 \* -  $p$ -value < 0.005 \*\*

Subsequently, we analysed intestinal mucosal integrity after DSS treatment and release (**Fig. 4.1**) in both *NCOA4* KO and WT mice by staining colon tissues with Hematoxylin & Eosin. *NCOA4* KO and WT mice both showed a completely disrupted intestinal mucosa after 7 days of treatment. Nevertheless, while WT mice displayed new intestinal crypts and regeneration of intestinal mucosa after 3 and 6 days of release from the treatment, *NCOA4* KO mice did not heal the damage induced by the treatment. In fact, in KO animals the intestinal tissue architecture was still altered with a decreased number of intestinal crypts after 3 days from release and this condition was still present also after 6 days (**Fig 4.3**).

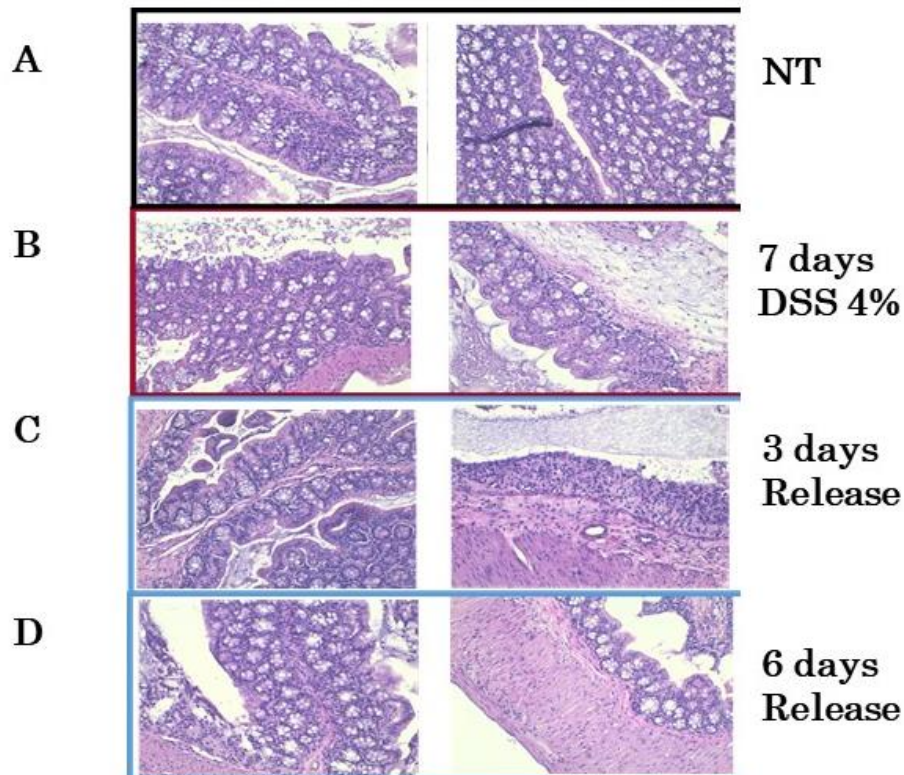


**Figure 4.3** Representative Hematoxylin & Eosin staining of colon sections from NCOA4 KO and WT mice.

**A** Intestinal section from not treated NCOA4 KO and WT mice are represented. **B.** After 7 days of DSS treatment colon sections from NCOA4 KO and WT mice displayed lack of intestinal mucosa architecture and destroyed crypts. **C.** After 3 days of release from the treatment WT mice displayed regenerated crypts while NCOA4 KO mice displayed loss of crypts structures. **D.** After 6 days from treatment release WT mice showed restored intestinal mucosa and crypt structures while NCOA4 KO mice still exhibited a low number of regenerated crypts and altered intestinal mucosa architecture

Based on the reduced colon regeneration displayed by NCOA4 KO mice, we further investigated proliferation levels of intestinal cells upon treatment with DSS and release. We performed an immunohistochemistry of colon sections with anti-phospho-Histone3 (p-H3) antibody which stains mitotic cells. We counted the number of mitotic cells (mean number of positive cells for each field 20X) and we found that the group of NCOA4 KO mice exhibited a reduced number of positive p-H3 cells compared to WT mice after 7 days of 4% DSS (**Fig 4.4 and 4.5**). Moreover, while WT mice presented an increase in the number of positive p-H3 cells after 3 and 6 days of release the NCOA4 KO mice still displayed a strong reduction in the number of positive p-H3 cells (**Fig 4.4 and 4.5**)

Overall, these results suggested that after the DSS treatment NCOA4 KO mice revealed an ineffective intestinal regeneration compared to the WT one.

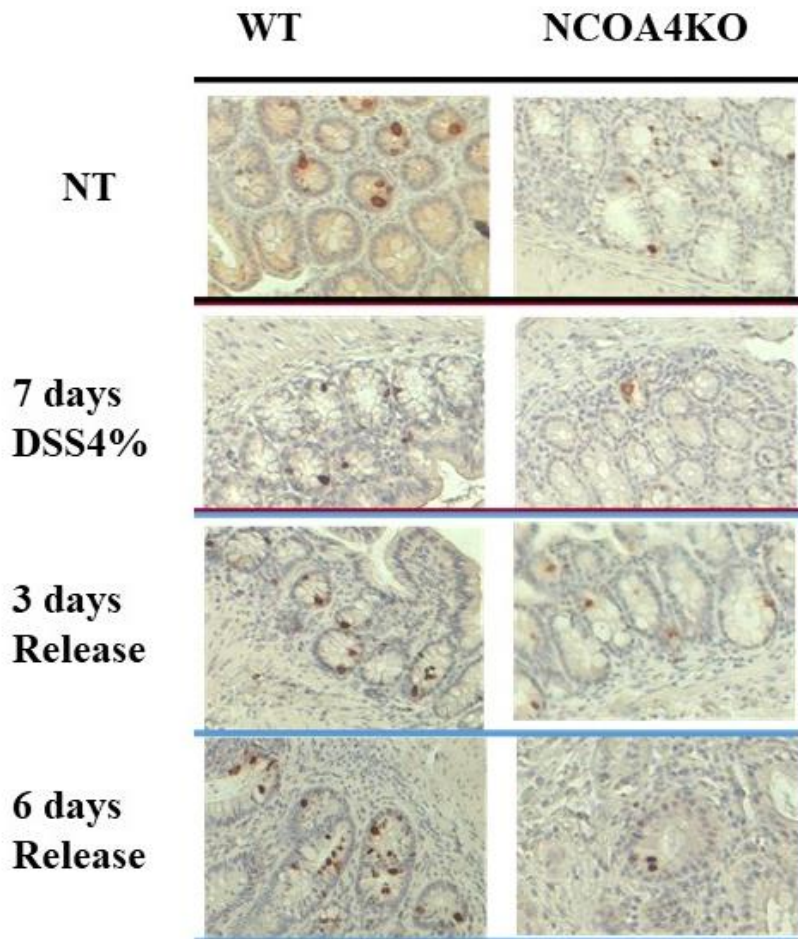


**Figure 4.4** Representative immunohistochemical staining for p-H3 of colon sections from NCOA4 KO and WT mice

As showed in the panels, after 7 days of treatment both groups of mice displayed reduced presence of p-H3 positive cells with respect to the NT groups of mice, with KO mice showing a stronger reduction compared to wt ones. After 3 and 6 days of release from the DSS treatment WT mice displayed an increased number of p-H3 positive cells with respect NCOA4 KO mice.

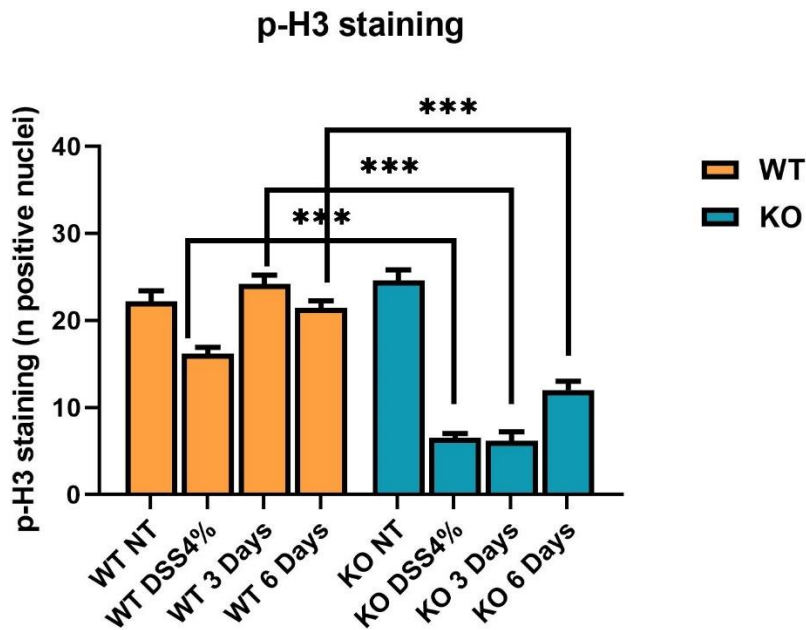
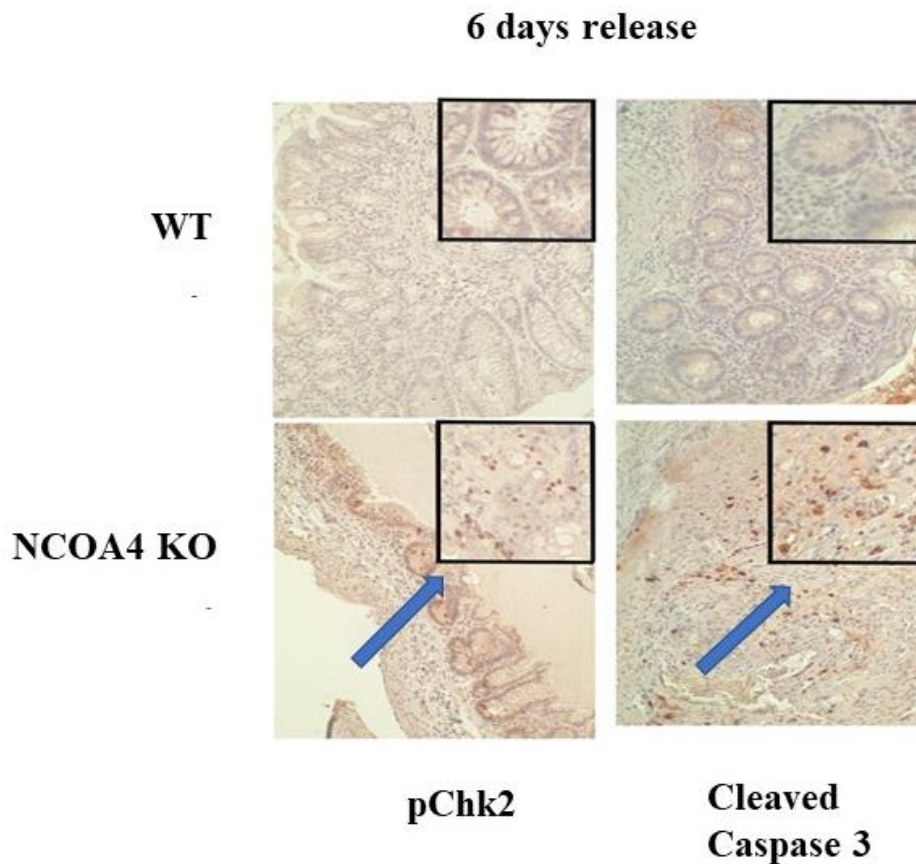


**Figure 4.5** *NCOA4* KO mice displayed reduced number of positive p-H3 cells after DSS4% treatment

Graphic representation of the pH3 positive cells after 7 days of DSS, and after 3 and 6 days of release from the treatment. As showed, *NCOA4* KO mice displayed a reduced number of positive p-H3 cells number respect to the WT mice during the experiment at each time point. The values were represented as Mean±SEM p-value < 0.0005\*\*\* (for each group 20 fields were counted)

Next, we investigated whether reduced proliferation of intestinal cells in *NCOA4* KO mice could be due to accumulation of DNA damage. To this aim, by immunohistochemistry we counted the number of cells positive for phosphorylation of Check-point kinase 2 (pChk2), a well-known marker of DNA damage (mean number of positive cells for each field 20X). We found that, differently from WT samples, colon sections of *NCOA4* KO mice displayed an elevated number of positive p-Chk2 cells still after 6 days of release (**Fig 4.6**). We also explored the presence of apoptotic cells, generally almost absent in normal intestinal mucosa, by performing an immunohistochemistry analysis for the apoptotic maker cleaved-caspase 3 (**Fig 4.6**). Differently from WT samples, after 6 days of release from the treatment colon section of *NCOA4* KO mice displayed an elevated number of cells that stained positive for cleaved-caspase 3 respect (**Fig 4.6**).

In conclusion, the proliferative stress induced by DSS treatment revealed that the absence of *NCOA4* in mice caused a reduced regeneration of intestinal tissue with activation of both DNA damage response and apoptotic pathways in intestinal cells.



**4.6 NCOA4 KO mice exhibited DNA damage and apoptosis.**

*Immunohistochemical staining for pChk2 and cleaved-Caspase3 of colon section from NCOA4 KO and WT mice after 6 days from DSS treatment. As showed, only the group of NCOA4 KO mice displayed a significant number of positive pChk2 and cleaved-Caspase3 cells compared to WT mice*

**4.2 NCOA4 KO mice exhibited defective intestinal stem cells proliferation**

After treatment with 4% DSS, NCOA4 KO mice displayed a phenotype characterized by strong reduction of colon length and disruption of intestinal mucosa with reduced presence of crypts, indicating an impaired ability to regenerate intestinal tissue. In this context, we decided to better elucidated whether the reduced intestinal regeneration of NCOA4 KO mice was due to defects in intestinal stem cells proliferation. Therefore, we analysed the expression levels of two intestinal stem cells marker: Lgr5 and BMI1. While Lgr5 is a marker of active stem cells, BMI1 represents a marker of quiescent stem cells. Both active and quiescent intestinal stem cells activate proliferation

upon tissue damage, to regenerate intestinal tissue. Thus, following the experimental scheme illustrated in **Figure 4.1**, we extracted RNA from NCOA4 KO and WT intestinal tissue and evaluated expression levels of Lgr5 and BMI1 by Real-Time PCR. We found that at basal levels both groups of mice showed a similar expression level of Lgr5 and BMI1. After 7 days of DSS treatment, both mouse strains showed a similar decreased expression of Lgr5 and BMI1. Interestingly, while WT mice started to increase expression of Lgr5 and BMI1 stem cell markers after 3 days from treatment release and reached normal levels of such markers after 6 days, NCOA4 KO mice completely failed to restore expression of both markers after 3 and 6 days from treatment release (**Fig 4.7-4.8**)

Hence, these results suggested that, after DSS treatment, WT mice activate intestinal stem cells proliferation to regenerate the intestinal damage, while NCOA4 KO mice fail to expand the Lgr5 and BMI1 positive intestinal stem cell pool, resulting in impaired regeneration of intestinal tissue.

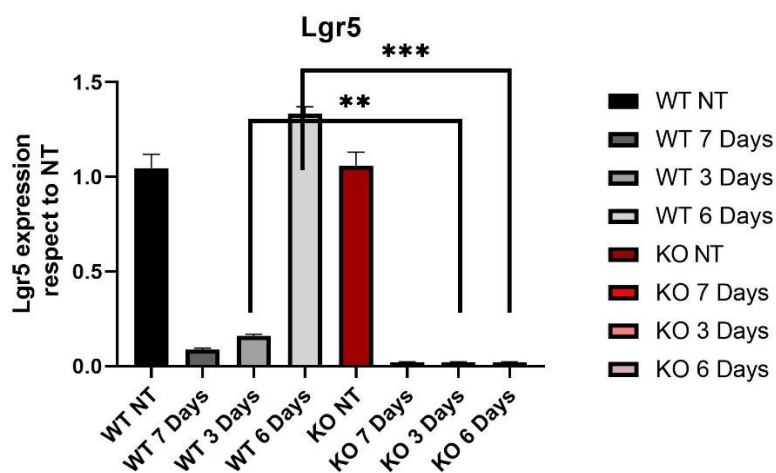


**Figure 4.7 NCOA4 KO mice displayed a reduced expression of Lgr5 mRNA.**

Lgr5 expression was measured by reverse-transcription polymerase chain reaction (RT-PCR). Samples were analysed in triplicate and normalized to the housekeeping gene GAPDH. NCOA4 KO mice exhibited a reduced expression of Lgr5 gene after 3 and 6 days of release from the treatment compared to WT mice. The values were represented as Mean±SEM p-value<0.005\*\* p value < 0.0005\*\*\*

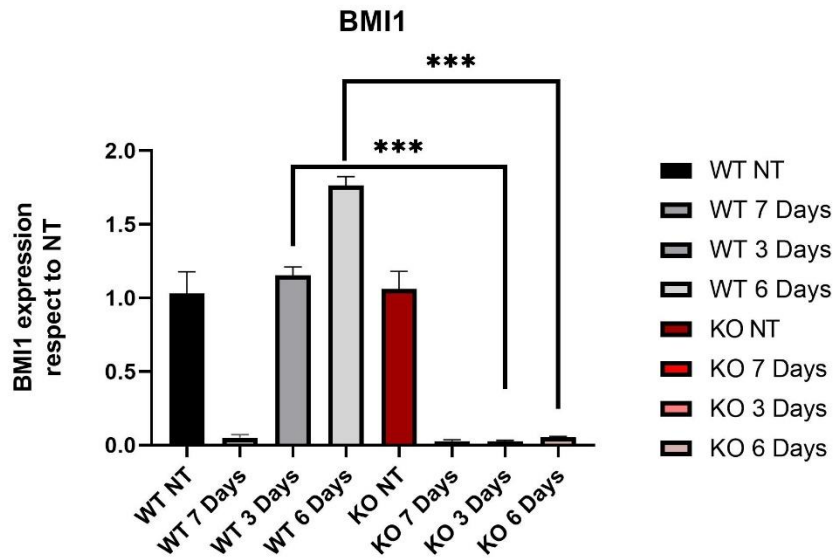


**Figure 4.8** *NCOA4* KO mice displayed a reduced expression of *BMI1* mRNA. *BMI1* expression was measured by reverse-transcription polymerase chain reaction (RT-PCR). Samples were analysed in triplicate and normalized to the housekeeping gene *GAPDH*. *NCOA4* KO mice exhibited a reduced expression of *BMI1* gene mice after 3 and 6 days of release from the treatment compared to WT mice. The values were represented as Mean ± SEM p value < 0.0005\*\*\*

### 4.3 *NCOA4* KO mice show a low survival after DSS 4% treatment

We explored whether the inability of *NCOA4* KO mice in regenerating intestinal mucosa upon DSS treatment resulted in a decreased survival of the animals. To this aim, we treated both *NCOA4* KO and WT mice with DSS for 7 days and then we followed animal survival. We observed a strong mortality rate in *NCOA4* KO mice, with all animals dying within 10 days from treatment release (**Fig 4.9**). On the contrary only 30% (2 out of 6) of WT mice group died after the treatment (**Fig 4.9**), indicating that the inability to recover from DSS injury resulted in a much lower survival for KO animals compared to WT ones and that *NCOA4* plays a relevant role in controlling tissue regeneration and proliferation *in vivo*.

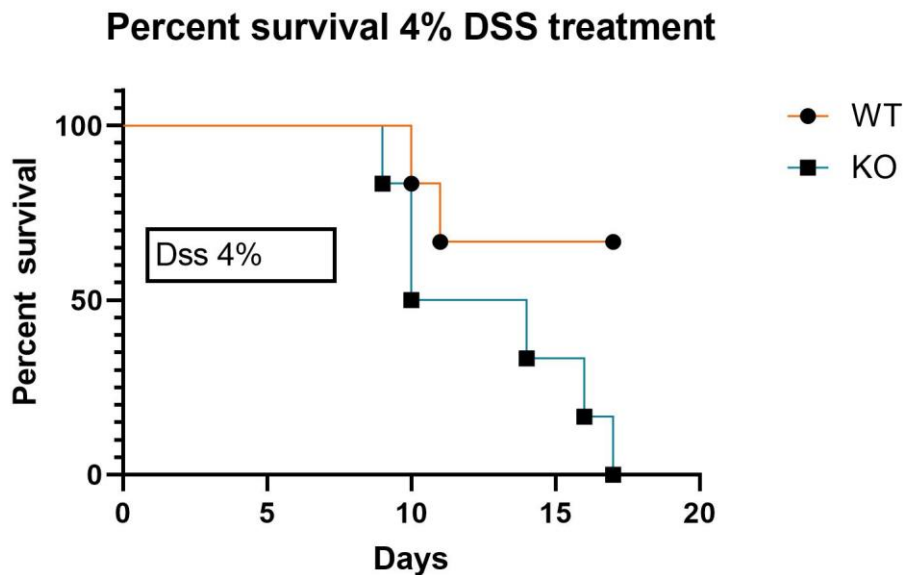


**Figure 4.9** *NCOA4 KO mice showed reduced survival after DSS4% treatment.*  
*NCOA4 KO and WT mice were treated for 7 days with DSS 4%. Survival of NCOA4 KO (blue) and WT (orange) mice is represented after the release from the DSS treatment. As showed, no mice survived in NCOA4 KO group while most (70%) WT mice survived after DSS treatment.*

#### **4.4 NCOA4 KO mice displayed impaired BM-derived cell proliferation**

We hypothesized that, beyond intestine, also other tissues could exhibit an ineffective proliferation upon tissue damage in NCOA4 KO mice compared to the WT mice. Thus, we focused our attention on the bone marrow. We first evaluated whether at the steady state bone marrow (BM)-derived cells from NCOA4 KO mice displayed a different proliferative phenotype compared to WT mice. BM-derived cells from both strains were collected and plated on a semisolid medium composed of methylcellulose, which allows hematopoietic progenitors growth due to the presence of several cytokines and growth factors such as IL-3, IL-6, Epo. After 10 days from plating, we noticed that, at basal levels, there was no difference in all-lineage progenitors' ability to form colonies between NCOA4 KO and WT mice (data not shown).

Based on this evidence, we decided to stimulate proliferation of BM-derived cells performing 4 serial bleedings (400  $\mu$ l every 3 days) in NCOA4 KO and WT mice (**Fig 4.10**) and analysed the capacity of BM progenitors to form colonies *ex vivo* in methylcellulose. Furthermore, to distinguish the formation of erythroid-lineage progenitors' colonies (BFU-E, CFU-E) from other hematopoietic progenitors we stained BM-derived colonies with Bendizine, a chemical agent that specifically binds to the heme group present in hemoglobin.

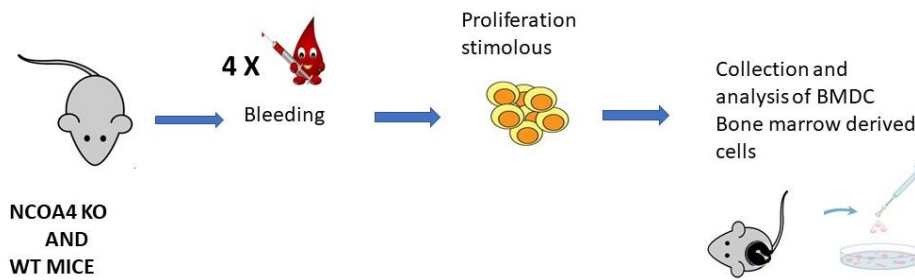


**Figure 4.10 Schematic representation of bleeding experiment in NCOA4 KO and WT mice.** Both groups of mice were subjected to 4 serial bleedings of 400 ul of blood each to stimulate proliferation of bone marrow precursors. Then BM-derived cells were collected from both group of mice and plated on semisolid medium (methylcellulose)

As shown in **Figure 4.11 and 4.12**, we found that NCOA4 KO mice not only displayed a lower number of colonies formed by all lineages progenitors compared to WT ones but also the erythroid-specific colonies (positive for benzidine staining), formed by BFU-E and CFU-E progenitors, were reduced in KO animals compared to compared WT.

These data indicate that under proliferative stress NCOA4 KO mice displayed an impaired tissue regeneration phenotype not only in the intestine but also in bone marrow

**BFU-E CFU-E Benzidine staining**

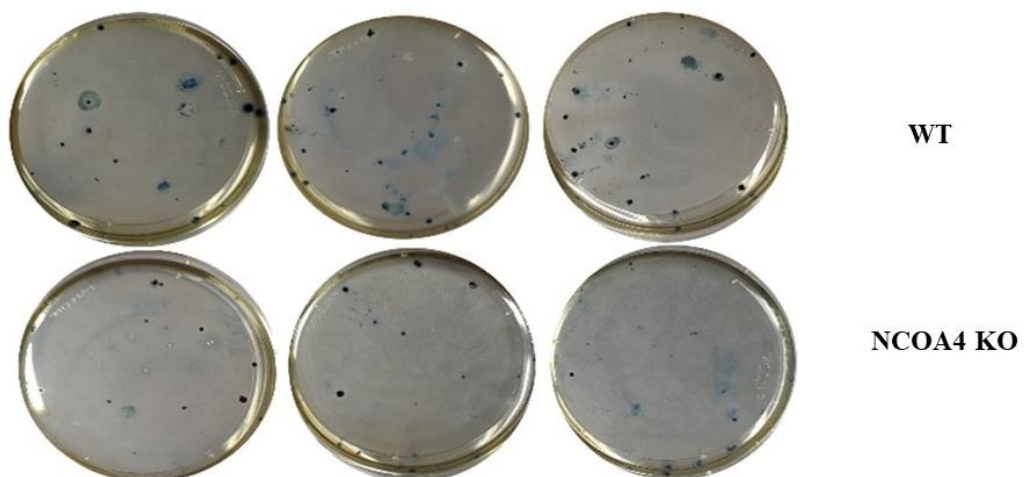


**Figure 4.11 NCOA4 KO mice showed impaired colony formation from BM-derived cells.** Representative picture of colony formation assay. BM-derived cells were plated on Methylcellulose. After 10 days erythroid-lineage colonies were stained with Benzidine (blue colonies) and counted. As showed, NCOA4 KO mice displayed decreased number of colonies respect to the WT group.

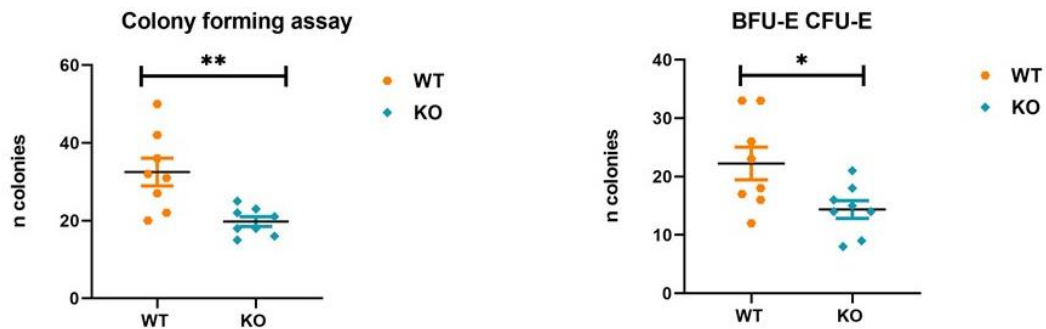


**Figure 4.12 NCOA4 KO mice displayed reduced number of BM-derived cells colonies.** Graphical representation of BM-derived cells colony assay of NCOA4 KO and WT mice. The graph on the left shows the number of total hematopoietic progenitors colonies derived from NCOA4 KO and WT mice. The graph on the right shows the number of erythroid-lineage colonies (benzidine positive) derived from NCOA4 KO and WT mice. The values were represented as Mean $\pm$ SEM p-value<0.05\*- p value < 0.005\*\*

#### 4.5 NCOA4 KO BM-derived cells and mice are sensitive to 5-FU treatment compared to WT cells and animals

Since the absence of NCOA4 in mice reduced proliferation of BM-derived cells after proliferative challenge, resulting in decreased colony forming ability of BM-derived cells, we next evaluated the colony forming capacity of BM-derived cells after administration of the genotoxic agent 5-fluorouracil (5-FU) *in vivo*. This compound is an analogous of uracil that inhibits the enzyme Thymidylate synthase resulting in activation of DNA damage response. When injected *in vivo*, 5-FU causes the ablation of hematopoietic precursors of bone marrow. This effect stimulates the proliferation of BM cells in response to the treatment. We administered 5-FU (100mg/Kg) to both NCOA4 KO and WT mice and then collected BM-derived cells. Cells were plated on methylcellulose as illustrated in the **Fig 4.13**. In order to evaluate self-renewal ability of BM-derived cells of both NCOA4 KO and WT mice we also performed serial replating in methylcellulose.

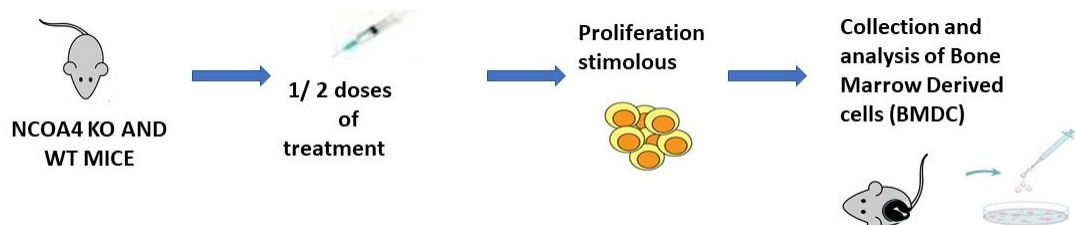


**Figure4.13 Representative scheme of 5-fluorouracil treatment in NCOA4 KO and WT mice.** We administered 1 dose of 5-FU (100mg/Kg) to induce proliferation stimulus. After 1 week from the treatment we collected and analyzed BM-derived cells.

After a single dose of 5-FU we observed that the number of colonies formed by BM-derived cells from NCOA4 KO and WT mice was the same in the first and in the 2 following replating (*Fig 4.14*).

Then to increase proliferative stress of bone marrow tissue, we treated NCOA4 KO and WT mice with 2 doses (1 dose weekly; 100mg/kg each dose) of 5-FU. We followed the experimental scheme (*Fig 4.13*) and counted the number of BM-derived cells formed colonies (*Fig 4.15*). While at the first plating NCOA4 KO and WT BM-derived cells showed a similar number of colonies, at the second and third replating NCOA4 KO mice exhibited a reduction of colonies compared to the WT mice (II replate Mean number: WT = 148.6 colonies/plate; NCOA4 KO= 105 colonies/plate p value <0,0005\*\*\*-III replate Mean number: WT= 45.3 colonies/plate; NCOA4= KO 8.3 colonies/plate p value <0,0005\*\*\*).

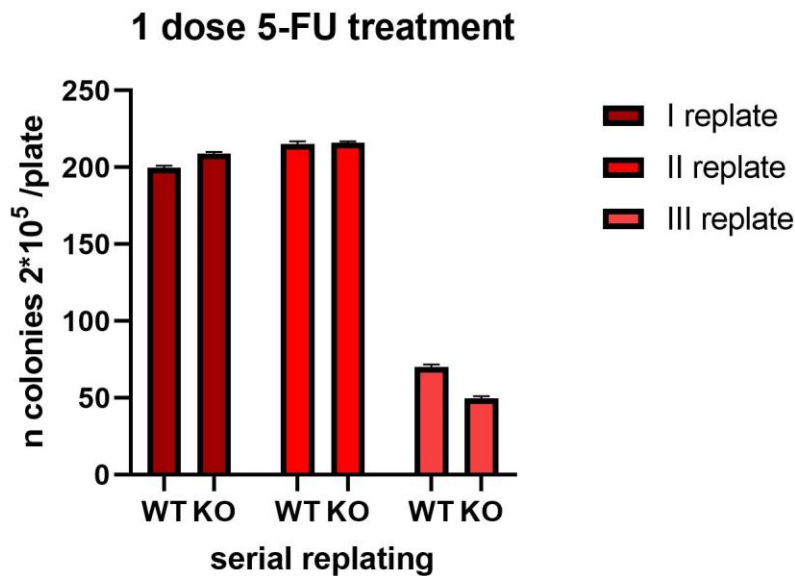


**Figure 4.14 A single dose of 5-FU did not affect BM-derived cells self-renewal.**

After the treatment with 1 dose of 5-FU,  $2 \times 10^5$  BM-derived cells were plated on methylcellulose. The graphs show the number of BM-derived colonies of NCOA4 KO and WT mice. Three serial replating were performed. The values were represented as Mean  $\pm$  SEM p value < 0.0005\*\*\*

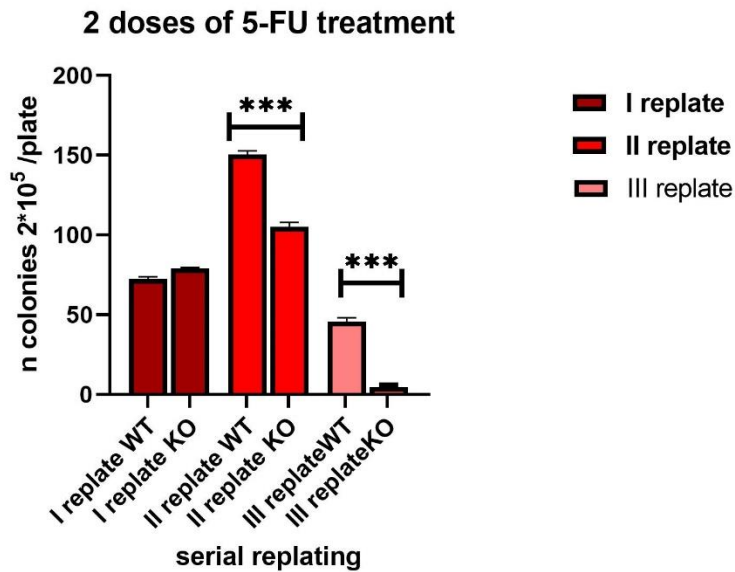


**Figure 4.15 2-doses of 5-FU treatment affected self-renewal ability of BM-derived cells**  
 After the treatment with 2 doses of 5-FU,  $2 \times 10^5$  BM-derived cells were plated on methylcellulose. The graphs show the number of BM-derived colonies of NCOA4 KO and WT groups of mice. In the second and third replating NCOA4 KO BM-derived cells showed a reduced number of colonies. The values were represented as Mean  $\pm$  SEM p value < 0.0005\*\*\*

Thus, 5-FU administration caused a regenerative response of BM tissue with a sustained self-renewal ability of BM-derived cells from WT mice. Conversely, the absence of NCOA4 in mice caused a reduced regenerative response probably due to affected self-renewal ability of BM-derived cells after 5-FU treatment. As mentioned before, NCOA4 KO mice revealed an impaired ability to form colonies after several replating upon 5-FU treatment. Based on this result we decided to better evaluate the relevance of damage induced by 5-FU treatment in NCOA4 KO mice compared to the WT one. We performed a survival experiment in both NCOA4 KO and WT mice treating them with a single dose of 5-FU weekly (**Fig 4.16**). We followed over time the vitality of both mice strains and observed that NCOA4 KO mice were more susceptible to the 5-FU treatment compared to the WT group. As a matter of fact, we observed that not only the NCOA4 KO mice started to die soon after the second 5-FU dose, but also that they all died within the second week of treatment (mean survival 12 days). On the contrary, WT mice started to die after 15 days from treatment start and not all animals died (4/6), reflecting a lower sensibility to the 5-FU treatment compared to NCOA4 KO mice. These results suggest that the presence of NCOA4 could be critical to regulate BM tissue regeneration and to avoid increased mortality upon genotoxic insult performed by 5-FU.

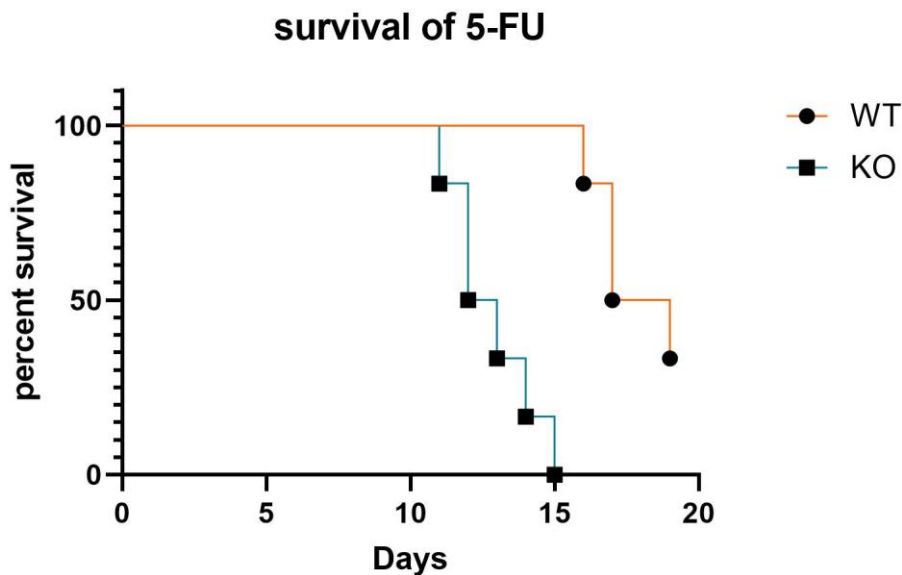


**Figure 4.16 NCOA4 KO mice showed a reduced survival upon 5-FU treatment**  
*NCOA4 KO and WT mice were treated with 5-FU every week (100mg/kg each dose). Survival of WT (orange) and NCOA4 KO (blue) mice is shown. After 15 days from treatment start all NCOA4 KO mice died. At day 20 from the treatment only 4 out of 6 WT mice died.*

#### **4.6 NCOA4 KO mice impaired tissue regeneration is not improved by iron supply**

Since regulation of DNA replication origins activation and iron availability is necessary for a correct cell cycle progression, and NCOA4 was demonstrated to regulate both these cellular process (Mancias, 2014, Bellelli, 2014, Federico, submitted), we asked which of these two NCOA4 functions was responsible for NCOA4 KO mice decreased tissue regeneration and survival upon insult with DSS.

Thus, we decided to perform an experiment by inducing regenerative response of intestinal cells with DSS, as previously described, but sustaining iron availability by injecting soluble iron dextran both in NCOA4 KO and WT mice. We wanted to evaluate whether complementing the absence of NCOA4 function in promoting ferritin degradation with iron dextran injection, NCOA4 KO mice were able to revert ineffective intestinal regeneration. To this aim, we treated mice for 7 days with 4 % DSS and injected iron dextran at day 0 and day 7 of DSS 4% treatment. Then we analysed intestinal tissue after 7 days of treatment and after 3 or 6 days of release from treatment (as illustrated in **Fig 4.17**)

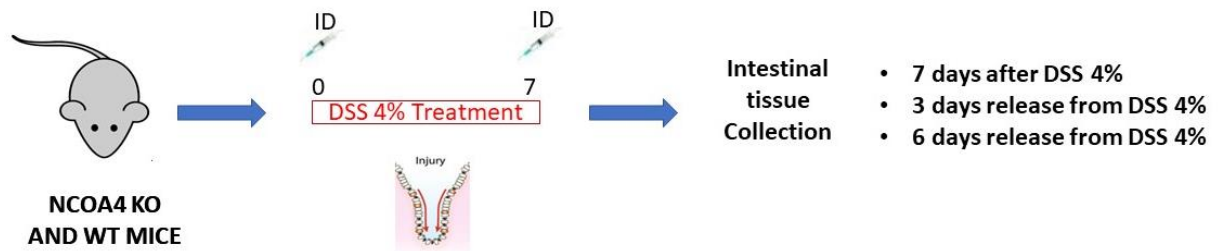


**Figure 4.17 Representative scheme of 4% DSS and iron dextran treatment in NCOA4 KO and WT mice.**

Mice were treated for 7 days dissolving DSS in drinking water. Iron dextran was injected the first and the last days of treatment. We collected intestinal tissue after 7 days of DSS treatment, and after 3 and 6 days of release from the treatment to analyse the regenerative response of both NCOA4 KO and WT mice.

We reasoned that iron dextran could improve iron availability in order to sustain tissue proliferation. To confirm that injected iron dextran increased iron availability, we evaluated Tf saturation levels over the time of the treatment (**Fig 4.18**). At day 7 we found that both NCOA4 KO and WT mice injected with iron dextran at day 0 and 7 increased Tf saturation up to 100% compared to the not treated animals which exhibited a normal Tf saturation about 50%. Interestingly, after 3 days of release, despite the iron dextran supply both group of mice showed a decreased Tf saturation, which reflected the condition of injury induced by DSS treatment. Decreased Tf saturation was particularly severe in NCOA4 KO mice not treated with iron dextran. These group of mice (KO not treated with iron dextran) still displayed a low Tf saturation after 6 days of release, while, at the same time point, NCOA4 KO and WT mice treated with iron dextran and WT treated mice not treated with iron dextran displayed a normal Tf saturation levels after 6 days from release.

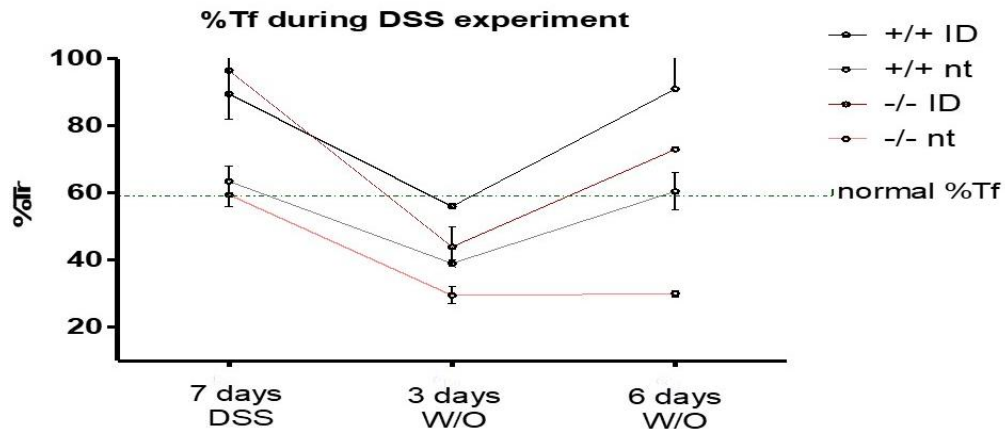


**Figure 4.18 Iron dextran improves serum Transferrin saturation during DSS 4% treatment**  
*NCOA4 KO and WT mice were subjected to peritoneal injections with 1 g per kg body weight of iron dextran (ID) at day 0 and 7 after the DSS treatment. The mice were sacrificed at the indicated time intervals and analyzed for transferrin saturation. At day 7 of DSS treatment Tf saturation is dramatically increased in both NCOA4 KO and WT mice treated with ID. At 3 days of release from the treatment WT and NCOA4 ID mice displayed a reduced Tf saturation. At 3 and 6 days of release NCOA4 KO mice not treated with ID showed a lower Tf saturation respect the all the other mice groups.*

Then, we evaluated whether increased iron availability and consequent Tf saturation improved regenerative intestinal response in NCOA4 KO and WT mice. Thus, we performed an immunohistochemical analysis of colon tissue of DSS treatment and after 3 and 6 days of release in WT and NCOA4 KO mice treated or not with iron dextran (ID) staining samples for the proliferative marker p-H3 (**Fig 4.19 and 4.20**) and we counted the number of positive p-H3 cells. The results confirmed that NCOA4 KO mice exhibited a low number of positive p-H3 cells compared to the WT group after DSS 4% treatment and after 3 and 6 days of treatment release. Interestingly ID treatment did not improve cell proliferation in either WT or NCOA4 KO mice.



We also performed an immunohistochemistry analysis to evaluate the presence of the apoptotic marker cleaved-caspase 3 in intestinal sections of both NCOA4 KO and WT mice treated or not with iron dextran (**Fig 4.21**). Again, we found that the number of positive cleaved-caspase 3 is higher in NCOA4 KO mice compared to the WT ones after DSS treatment. Furthermore, we noticed that there were no differences in the number of positive cleaved-caspase 3 cells between the group of NCOA4 KO mice treated or not with iron dextran (**Fig 4.22**). The increased presence of apoptotic cells in intestinal tissue of NCOA4 KO mice despite the increased Tf saturation was in accordance with the reduced presence of proliferative intestinal cells evaluated previously in the same iron supply condition

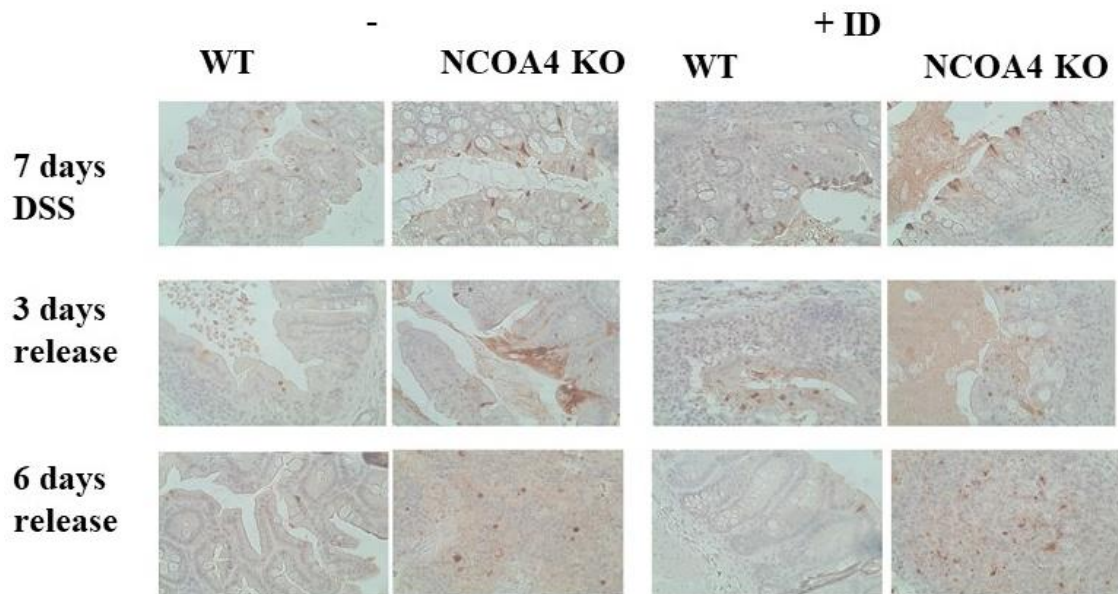


**Figure 4.21 Cleaved-caspase3 immunohistochemical staining**

As showed in the panel NCOA4 KO treated or not with iron dextran mice showed a similar number of cleaved-caspase 3 positive cells after 7 days of treatment and after 3 and 6 days of release from the treatment

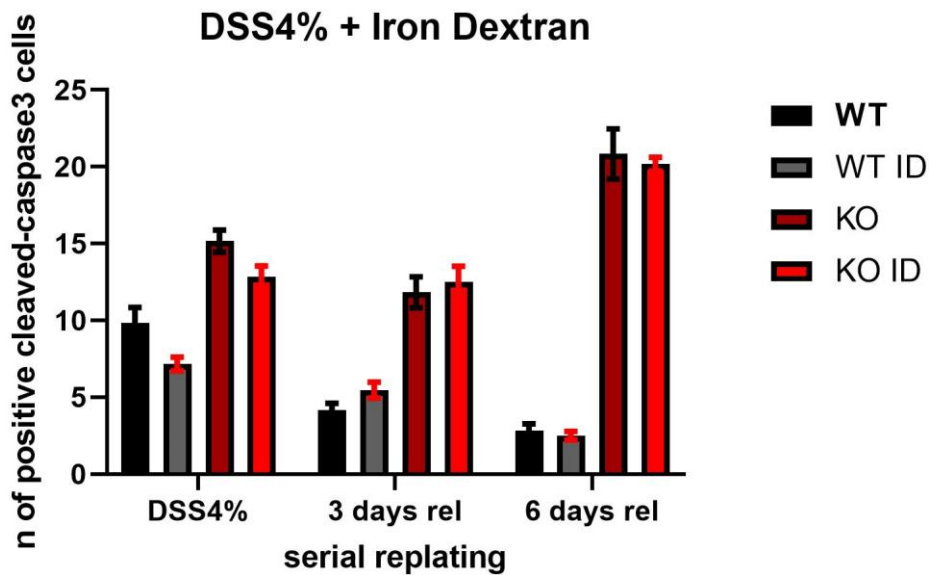


**Figure 4.22 Evaluation of cleaved-caspase 3 positive cells after DSS4% +/- ID treatment**  
 Quantification of cleaved-caspase3 positive cells in intestinal sections of NCOA4 KO and WT mice after DSS 4% treatment and after 3 or 6 days of release treated or not with ID. As showed in the graph at 7 days of DSS treatment the group of NCOA4 KO and NCOA4 KO ID showed a similar number of positive cleaved-caspase3 positive cells. Similarly, after 3 or 6 days of release from the treatment NCOA4 KO and NCOA4 KO ID mice displayed no significant difference in the number of cleaved-caspase 3 positive cells.

Overall, these data suggested that an increase in Tf saturation did not improve the impairment of intestinal tissue regeneration displayed in absence of NCOA4 in mice indicating that NCOA4 KO phenotype was not due mainly to the reduced iron levels, but to the absence of NCOA4 function in controlling activation of DNA origins replication.

#### 4.7 The absence of NCOA4 in low iron condition did not affect Iron-Sulfur (Fe-S) cluster proteins levels

To better sustain our hypothesis that it was the absence of NCOA4 function in controlling DNA replication origin activation responsible for reduced proliferation both in cells and mice and not ferritinophagy impairment, we decided to evaluate the protein levels of specific iron-sulfur (Fe-S) cluster enzymes. Thus, Fe-S cluster enzymes require iron as a cofactor and are essential for the correct progression of DNA replication.

We first evaluated the Labile Iron Pool (LIP) of both NCOA4 silenced (shNCOA4) and control (shCTR) cells and we found that shNCOA4 cells exhibited a lower LIP concentration compared to shCTR cells (**Fig 4.23**). This is in accordance with the absence of NCOA4 function in controlling ferritin

degradation and consequent decreased iron release. As a consequence, HeLa cells silenced for NCOA4 showed increased levels of TfR1 and IRP2 compared to the control cells at basal levels (**Fig 4.24**). Then, we induced a strong and acute iron deprivation by treating cells with iron chelator deferoxamine (DFO) for 2 or 24h. Both cell types upregulated TfR1 and IRP2 after 24 hours, compared to untreated cells (**Fig 4.24**). These results indicated that cells lacking NCOA4-mediated ferritinophagy compensated the condition of low iron levels by increasing TfR1 and IRP2 protein levels.

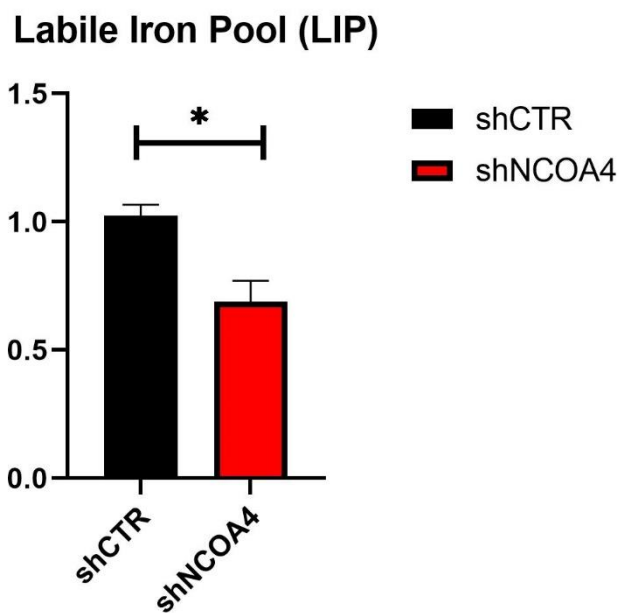


**Figure 4.23 HeLa shNCOA4 showed reduced LIP**

Labile iron pool was evaluated in HeLa shCTR and shNCOA4 by Calcein staining.

As showed in the graph, the absence of NCOA4 in cells affected LIP levels respect to shCTR cells. The values were represented as Mean $\pm$ SEM p-value<0.05\*

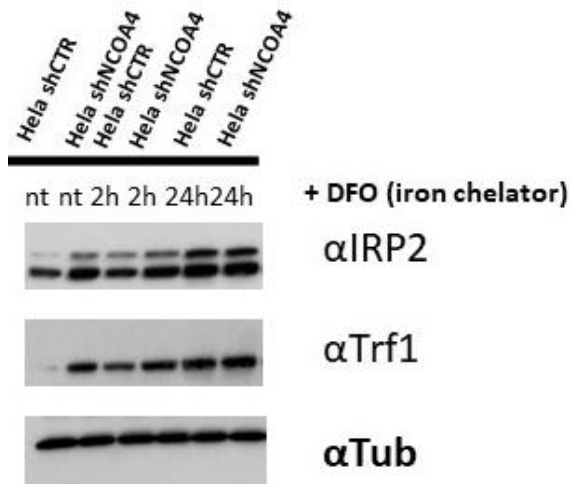


**Figure 4.24** Loss of NCOA4 in HeLa cells increased IRP2 and Trf1 levels. WB analysis revealed that HeLa cells silenced for NCOA4 protein, showed increased levels of IRP2 and Trf1 levels respect to shCTR at steady state. After 2h of DFO treatment HeLa shCTR showed increased levels of Trf1 and IRP2 respect to the steady state and Trf1 and IRP2 levels were similar between HeLa shNCOA4 and shCTR cells.

Then we performed a western blot analysis to determine protein levels of Fe-S cluster containing proteins such as DNA Polymerases Delta (PolD) and helicases FNCJ and XPD, both at the steady state and upon iron deprivation induced by DFO treatment for 2 or 24 hours (**Fig 4.25**). We noticed that both at the steady state and after 2 or 24 hours of DFO treatment no difference in Fe-S cluster enzymes were observed between shCTR and shNCOA4 cells. Since Ribonucleotide Reductase (RNR) also uses iron as cofactor to produce dNTPs, we also evaluated its levels both in shCTR and shNCOA4 cells upon treatment of 2 or 24 hours with DFO (**Fig 4.26**). Thus, by performing a WB analysis for ribonucleotide reductase subunit 1 (RRM1) and subunit 2 (RRM2) we noticed that RRM1 and RMM2 protein levels were the same in shNCOA4 and shCTR cells at the steady state and after 2h or 24 h DFO treatment.

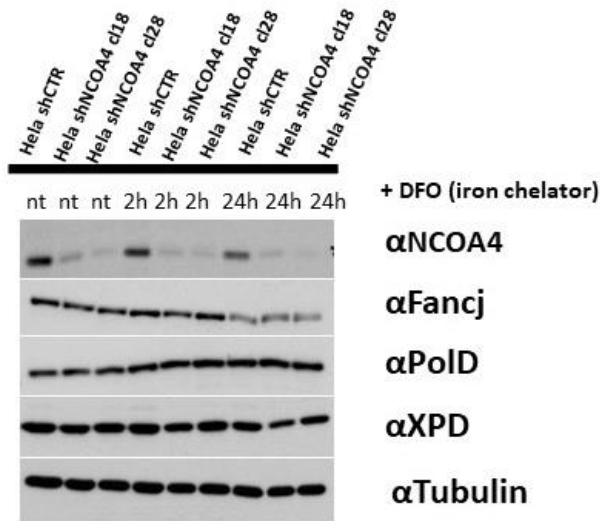


**Figure 4.25** *The absence of NCOA4 does not impaired Fe-S cluster enzymes protein levels*  
 As showed in the panel, shCTR and shNCOA4 cells showed similar Fancj, PolD and XPD protein levels both at basal levels and after 2h or 24 h of DFO treatment.

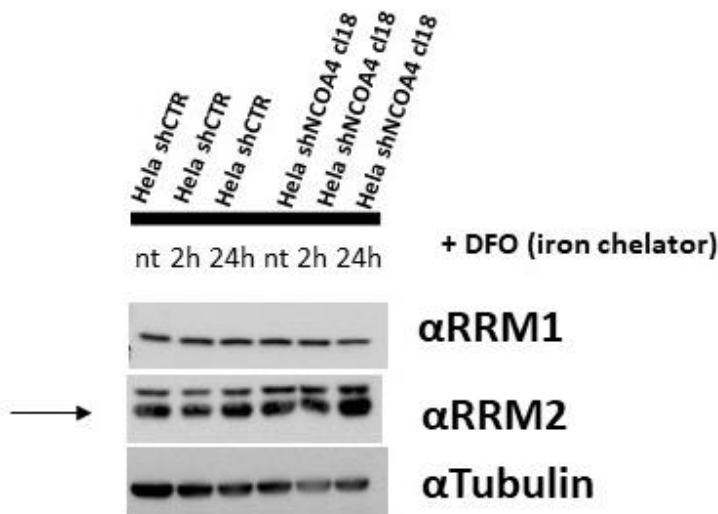


**Figure 4.26** *The absence of NCOA4 does not impaired Ribonucleotide Reductase (RNR) protein levels*  
 As showed in the panel, shCTR and shNCOA4 cells showed similar Ribonucleotide Reductase portion 1 and 2 protein levels both at basal levels and after 2h or 24 h of DFO treatment

Finally, this data also suggested that the phenotype of reduced proliferation and DNA damage activation observed in cells without NCOA4 was due mainly to the absence of nuclear function of NCOA4 (regulation of DNA origins activation) and was not indirectly depended on low intracellular iron levels due to the absence of cytosolic NCOA4 function (regulation of ferritin degradation).

## 5. DISCUSSION

The Nuclear Receptor CoActivator 4 inhibits DNA replication origin activation by binding the MCM7 protein, member of the DNA helicase complex (MCM2-7). Through this interaction NCOA4 hinders the activation of DNA replication origins, during the process also known as origin “firing” which occurs during the S phase of the cell cycle (Bellelli et al. 2014). Moreover, NCOA4 exhibits a cytosolic function. Indeed, NCOA4 regulates intracellular iron levels by binding ferritin, and promoting its lysosomal degradation and consequent iron release (Mancias et al. 2014). NCOA4 is an iron binding protein, and thanks to this characteristic its intracellular levels are regulated by an E3-ubiquitin ligase, also known as HERC2, in an iron-dependent manner. Indeed, under iron replete condition NCOA4 binds iron and is recognized by HERC2 which promotes its proteasomal degradation (Mancias et al. 2015).

Iron represents an essential microelement for several cellular processes; particularly, iron is essential to ensure a correct DNA replication and cell cycle progression so that low iron levels induce a G1/S cell cycle arrest (Le 2002). Several enzymes involved in DNA metabolism and repair require iron as a cofactor (C. Zhang 2014). Since iron represents an essential microelement for DNA synthesis and NCOA4 regulates both intracellular iron levels and DNA replication activation, we hypothesized that intracellular iron levels regulate both NCOA4 functions to restrain DNA replication and promote ferritin degradation in iron depletion. Our preliminary data confirmed that low iron concentration not only promoted NCOA4-mediated ferritin degradation but also NCOA4 binding onto chromatin. Hence, upon iron deprivation NCOA4 acts an iron sensor and increases its binding onto chromatin to interact with MCM7 protein in order to inhibit the activation of DNA replication origins, avoid uncontrolled DNA replication and consequent accumulation of DNA damage. Indeed, upon iron deprivation, loss of NCOA4 in cells not only causes unscheduled DNA replication origin activation but also increases signs of replication stress and DNA damage compared to WT cells (Federico et al, submitted).

Here we investigate the relevance of NCOA4 in coupling DNA replication to iron levels *in vivo* by using NCOA4 KO mice. We focused on the intestinal tissue that undergoes continuous turnover to replenish lost cells through the activity of proliferating stem cells present into the intestinal crypts (Buczacki et al. 2013). Thus, we evaluated the regenerative capacity of intestinal mucosa upon damage induced by Sodium Dextran Sulfate both in NCOA4 KO and WT mice. Interestingly, we found that WT animals were able to recover from the DSS-dependent intestinal damage, resulting in complete regeneration of intestinal tissue and crypt structure in 6 days, whereas the absence of NCOA4 in mice caused an impaired recover from the DSS-mediated intestinal damage. Thus, we found presence of DNA damage and consequent activation of apoptosis in NCOA4 KO intestinal mucosa.

The reduced regeneration and presence of DNA damage and apoptosis exhibited by NCOA4 KO mice are in accordance with the absence of NCOA4 function in

controlling DNA replication as demonstrated *in vitro* (Federico submitted). Likely, the absence of DNA replication blockade exerted by NCOA4 causes an unscheduled DNA replication origins activation that results in reduced intestinal stem cells proliferation due to DNA damage and apoptosis. Intestinal stem cells require a finely regulation of DNA replication to sustain the high renewing of intestinal tissue (Simons and Clevers 2011). NCOA4 function in controlling DNA replication origin activation could be necessary to ensure a correct cell proliferation in intestinal stem cells. Thus, we demonstrated that the absence of NCOA4 affects the expression of Lgr5<sup>+</sup> and BMI1 markers of the intestinal stem cells which are responsible for the rapid renewing of intestinal epithelium (Basak et al. 2014) (Buczacki et al. 2013). The reduced proliferation of intestinal stem cells strongly affected intestinal regeneration and finally lead to poor survival of NCOA4 KO mice compared to WT ones.

Our results indicate that absence of NCOA4 in mice also affects bone marrow regeneration. Notably, the bone marrow tissue is characterized by the presence of highly proliferating progenitors, as well as quiescent stem cells, also known as Hematopoietic Stem Cells (HSCs), which are activated upon proliferation stress (Sun et al. 2014) (Busch et al. 2015). HSCs are cells with characteristics of pluripotency and self-renewal that are capable of generating an entire hematopoietic system (Sun et al. 2014).

NCOA4 KO mice showed ineffective colony formation ability of BM-derived cells after inducing a proliferative stimulus by mice serial bleeding or repeated bone marrow insult by 5-Fluorouracil. Interestingly, we found that not only the differentiated erythroid lineage was affected, but also the total myeloid lineage. These results suggested that the reduced BM-derived cells proliferation in NCOA4 KO mice may be due to impaired differentiation or ineffective proliferation of HSCs progenitors. This condition makes NCOA4 KO mice unable to recover from repeated doses of 5-FU treatment exhibiting a strong mortality upon treatment compared to WT mice. Evidence that DNA damage plays a causal role in the aging process includes the observation that mice with defects in DNA replication and DNA damage repair display aspects of premature aging (Freitas and de Magalhães 2011). We suspect that the absence of NCOA4 function in controlling DNA replication affects genome stability of progenitor stem cells resulting in reduced proliferation capacity which is a characteristic of aged stem cell phenotype.

Besides its role in regulating ferritin degradation, NCOA4 could also support DNA replication indirectly sustaining the production and function of several enzymes such as Fe-S cluster enzymes and Ribonucleotide Reductase which requires iron as cofactor. Hence, we asked whether upon low iron condition NCOA4-mediated ferritin degradation could represent a source for iron availability. Our results demonstrated that the absence of NCOA4 in cells did not affect the intracellular levels of both Fe-S cluster enzymes and Ribonucleotide Reductase. These findings indicate that NCOA4 regulation of iron availability is not indispensable and that cells are able to supply iron levels

through the increased expression of iron regulatory protein such as TfR1 and IRP2.

Moreover, we also demonstrated that the phenotype of impaired tissue regeneration displayed by NCOA4 KO mice is not reverted by iron supply during DSS treatment, indicating that the function of NCOA4 in controlling DNA origins activation is mainly responsible for the reduced tissue regeneration. Overall, our findings indicate that NCOA4 plays a crucial role in regulating cellular proliferation. NCOA4 function in regulating DNA replication origin activation is essential to mediate both a correct proliferation *in vitro* and tissue regeneration *in vivo*. The NCOA4 control of DNA replication may represent a new mechanism of control when iron levels are not sufficient to ensure a correct proliferation and consequent genome stability

## 6. CONCLUSIONS

To ensure a correct tissue proliferation, iron levels and DNA replication need to be coordinated, particularly for high proliferative tissues. In this study we demonstrated that NCOA4 regulation of DNA replication origin activation is essential to promote intestinal and bone marrow regeneration after a proliferative stress. Indeed, our data showed that lack of NCOA4 function strongly affects the staminal pool of both intestinal and bone marrow tissue. Thus, NCOA4 is crucial to avoid replication stress and accumulation of DNA damage which cause cellular death and impaired regeneration *in vivo*.

Our study provides a new mechanism of regulation of DNA replication activation and iron availability in which NCOA4 acts as a key regulator.

## References

- Aisen, Philip. 2004. «Transferrin Receptor 1». *The International Journal of Biochemistry & Cell Biology* 36 (11): 2137–43.
- Alcantara, O. 2001. «Expression of multiple genes regulating cell cycle and apoptosis in differentiating hematopoietic cells is dependent on iron». *Experimental Hematology* 29 (9): 1060–69.
- An, Xiuli, Vincent P. Schulz, Jie Li, Kunlu Wu, Jing Liu, Fumin Xue, Jingping Hu, Narla Mohandas, e Patrick G. Gallagher. 2014. «Global Transcriptome Analyses of Human and Murine Terminal Erythroid Differentiation». *Blood* 123 (22): 3466–77.
- Arosio, Paolo, Leonardo Elia, e Maura Poli. 2017. «Ferritin, Cellular Iron Storage and Regulation». *IUBMB Life* 69 (6): 414–22.
- Arosio, Paolo, Rosaria Ingrassia, e Patrizia Cavadini. 2009. «Ferritins: A Family of Molecules for Iron Storage, Antioxidation and More». *Biochimica et Biophysica Acta (BBA) - General Subjects* 1790 (7): 589–99.
- Babitt, Jodie L, Franklin W Huang, Diedra M Wrighting, Yin Xia, Yisrael Sidis, Tarek A Samad, Jason A Campagna, et al. 2006. «Bone Morphogenetic Protein Signaling by Hemojuvelin Regulates Hepcidin Expression». *Nature Genetics* 38 (5): 531–39.
- Basak, Onur, Maaike Born, Jeroen Korving, Joep Beumer, Stefan Elst, Johan H Es, e Hans Clevers. 2014. «Mapping Early Fate Determination in L Gr5<sup>+</sup> Crypt Stem Cells Using a Novel *K 167- RFP* Allele». *The EMBO Journal* 33 (18): 2057–68.
- Bellelli, Roberto, Maria Domenica Castellone, Teresa Guida, Roberto Limongello, Nina Alayne Dathan, Francesco Merolla, Anna Maria Cirafici, et al. 2014. «NCOA4 Transcriptional Coactivator Inhibits Activation of DNA Replication Origins». *Molecular Cell* 55 (1): 123–37.
- Bellelli, Roberto, Giorgia Federico, Alessandro Matte', David Colecchia, Achille Iolascon, Mario Chiariello, Massimo Santoro, Lucia De Franceschi, e Francesca Carlomagno. 2016. «NCOA4 Deficiency Impairs Systemic Iron Homeostasis». *Cell Reports* 14 (3): 411–21.
- Bowers, Jayson L., John C.W. Randell, Shuyan Chen, e Stephen P. Bell. 2004. «ATP Hydrolysis by ORC Catalyzes Reiterative Mcm2-7 Assembly at a Defined Origin of Replication». *Molecular Cell* 16 (6): 967–78.
- Buczacki, Simon J. A., Heather Ireland Zecchini, Anna M. Nicholson, Roslin Russell, Louis Vermeulen, Richard Kemp, e Douglas J. Winton. 2013. «Intestinal Label-Retaining Cells Are Secretory Precursors Expressing Lgr5». *Nature* 495 (7439): 65–69.
- Busch, Katrin, Kay Klapproth, Melania Barile, Michael Flossdorf, Tim Holland-Letz, Susan M. Schlenner, Michael Reth, Thomas Höfer, e Hans-Reimer Rodewald. 2015. «Fundamental Properties of

- Unperturbed Haematopoiesis from Stem Cells in Vivo». *Nature* 518 (7540): 542–46.
- Canonne-Hergaux, F., S. Gruenheid, P. Ponka, e P. Gros. 1999. «Cellular and Subcellular Localization of the Nramp2 Iron Transporter in the Intestinal Brush Border and Regulation by Dietary Iron». *Blood* 93 (12): 4406–17.
- Carr, A. M. 2000. «CELL CYCLE:Piecing Together the p53 Puzzle». *Science* 287 (5459): 1765–66.
- Castillo, Jonathan P., Fiona M. Frame, Harry A. Rogoff, Mary T. Pickering, Andrew D. Yurochko, e Timothy F. Kowalik. 2005. «Human Cytomegalovirus IE1-72 Activates Ataxia Telangiectasia Mutated Kinase and a P53/P21-Mediated Growth Arrest Response». *Journal of Virology* 79 (17): 11467–75.
- Coverley, D., C. Pelizon, S. Trewick, e R. A. Laskey. 2000. «Chromatin-Bound Cdc6 Persists in S and G2 Phases in Human Cells, While Soluble Cdc6 Is Destroyed in a Cyclin A-Cdk2 Dependent Process». *Journal of Cell Science* 113 ( Pt 11): 1929–38.
- Donovan, Adriana, Alison Brownlie, Yi Zhou, Jennifer Shepard, Stephen J. Pratt, John Moynihan, Barry H. Paw, et al. 2000. «Positional Cloning of Zebrafish Ferroportin1 Identifies a Conserved Vertebrate Iron Exporter». *Nature* 403 (6771): 776–81.
- Du, X., E. She, T. Gelbart, J. Truksa, P. Lee, Y. Xia, K. Khovananth, et al. 2008. «The Serine Protease TMPRSS6 Is Required to Sense Iron Deficiency». *Science* 320 (5879): 1088–92.
- Fragkos, Michalis, Olivier Ganier, Philippe Coulombe, e Marcel Méchali. 2015. «DNA Replication Origin Activation in Space and Time». *Nature Reviews Molecular Cell Biology* 16 (6): 360–74.
- Freitas, Alex A., e João Pedro de Magalhães. 2011. «A Review and Appraisal of the DNA Damage Theory of Ageing». *Mutation Research/Reviews in Mutation Research* 728 (1–2): 12–22.
- Heller, Ryan C., Sukhyun Kang, Wendy M. Lam, Shuyan Chen, Clara S. Chan, e Stephen P. Bell. 2011. «Eukaryotic Origin-Dependent DNA Replication In Vitro Reveals Sequential Action of DDK and S-CDK Kinases». *Cell* 146 (1): 80–91.
- Higa, Mitsunori, Masatoshi Fujita, e Kazumasa Yoshida. 2017. «DNA Replication Origins and Fork Progression at Mammalian Telomeres». *Genes* 8 (4): 112.
- Kakhlon, Or, e Z. Ioav Cabantchik. 2002. «The Labile Iron Pool: Characterization, Measurement, and Participation in Cellular Processes». *Free Radical Biology and Medicine* 33 (8): 1037–46.
- Kollara, Alexandra, e Theodore J. Brown. 2012. «Expression and Function of Nuclear Receptor Co-Activator 4: Evidence of a Potential Role Independent of Co-Activator Activity». *Cellular and Molecular Life Sciences* 69 (23): 3895–3909.

- Kruszewski, M. 2003. «Labile Iron Pool: The Main Determinant of Cellular Response to Oxidative Stress». *Mutation Research/Fundamental and Molecular Mechanisms of Mutagenesis* 531 (1–2): 81–92.
- Kumar, Dinesh, Jörgen Viberg, Anna Karin Nilsson, e Andrei Chabes. 2010. «Highly Mutagenic and Severely Imbalanced DNTP Pools Can Escape Detection by the S-Phase Checkpoint». *Nucleic Acids Research* 38 (12): 3975–83.
- Lane, D.J.R., A.M. Merlot, M.L.-H. Huang, D.-H. Bae, P.J. Jansson, S. Sahni, D.S. Kalinowski, e D.R. Richardson. 2015. «Cellular Iron Uptake, Trafficking and Metabolism: Key Molecules and Mechanisms and Their Roles in Disease». *Biochimica et Biophysica Acta (BBA) - Molecular Cell Research* 1853 (5): 1130–44.
- Le, N. 2002. «The Role of Iron in Cell Cycle Progression and the Proliferation of Neoplastic Cells». *Biochimica et Biophysica Acta (BBA) - Reviews on Cancer* 1603 (1): 31–46.
- Leonard, A. C., e M. Mechali. 2013. «DNA Replication Origins». *Cold Spring Harbor Perspectives in Biology* 5 (10): a010116–a010116.
- Lill, Roland. 2009. «Function and Biogenesis of Iron–Sulphur Proteins». *Nature* 460 (7257): 831–38.
- Mancias, Joseph D., e Alec C. Kimmelman. 2016. «Mechanisms of Selective Autophagy in Normal Physiology and Cancer». *Journal of Molecular Biology* 428 (9): 1659–80.
- Mancias, Joseph D, Laura Pontano Vaites, Sahar Nissim, Douglas E Biancur, Andrew J Kim, Xiaoxu Wang, Yu Liu, Wolfram Goessling, Alec C Kimmelman, e J Wade Harper. 2015. «Ferritinophagy via NCOA4 Is Required for Erythropoiesis and Is Regulated by Iron Dependent HERC2-Mediated Proteolysis». *ELife* 4: e10308.
- Mancias, Joseph D., Xiaoxu Wang, Steven P. Gygi, J. Wade Harper, e Alec C. Kimmelman. 2014. «Quantitative Proteomics Identifies NCOA4 as the Cargo Receptor Mediating Ferritinophagy». *Nature* 509 (7498): 105–9.
- Masai, Hisao, Seiji Matsumoto, Zhiying You, Naoko Yoshizawa-Sugata, e Masako Oda. 2010. «Eukaryotic Chromosome DNA Replication: Where, When, and How?» *Annual Review of Biochemistry* 79 (1): 89–130.
- McKie, A. T. 2001. «An Iron-Regulated Ferric Reductase Associated with the Absorption of Dietary Iron». *Science* 291 (5509): 1755–59.
- Muckenthaler, Martina U., Stefano Rivella, Matthias W. Hentze, e Bruno Galy. 2017. «A Red Carpet for Iron Metabolism». *Cell* 168 (3): 344–61.
- Nemeth, E. 2004. «Hepcidin Regulates Cellular Iron Efflux by Binding to Ferroportin and Inducing Its Internalization». *Science* 306 (5704): 2090–93.
- Netz, Daili J A, Carrie M Stith, Martin Stümpfig, Gabriele Köpf, Daniel Vogel, Heide M Genau, Joseph L Stodola, Roland Lill, Peter M J Burgers, e Antonio J Pierik. 2012. «Eukaryotic DNA Polymerases Require an

- Iron-Sulfur Cluster for the Formation of Active Complexes». *Nature Chemical Biology* 8 (1): 125–32.
- Ohgami, Robert S, Dean R Campagna, Eric L Greer, Brendan Antiochos, Alice McDonald, Jing Chen, John J Sharp, Yuko Fujiwara, Jane E Barker, e Mark D Fleming. 2005. «Identification of a Ferrireductase Required for Efficient Transferrin-Dependent Iron Uptake in Erythroid Cells». *Nature Genetics* 37 (11): 1264–69.
- Pantopoulos, Kostas. 2004. «Iron Metabolism and the IRE/IRP Regulatory System: An Update». *Annals of the New York Academy of Sciences* 1012 (1): 1–13.
- Papanikolaou, G., e K. Pantopoulos. 2005. «Iron Metabolism and Toxicity». *Toxicology and Applied Pharmacology* 202 (2): 199–211.
- Papanikolaou, George, e Kostas Pantopoulos. 2017. «Systemic Iron Homeostasis and Erythropoiesis». *IUBMB Life* 69 (6): 399–413.
- Puig, Sergi, Lucía Ramos-Alonso, Antonia María Romero, e María Teresa Martínez-Pastor. 2017. «The Elemental Role of Iron in DNA Synthesis and Repair». *Metallomics* 9 (11): 1483–1500.
- Santoro, M., N. A. Dathan, M. T. Berlingieri, I. Bongarzone, C. Paulin, M. Grieco, M. A. Pierotti, G. Vecchio, e A. Fusco. 1994. «Molecular Characterization of RET/PTC3; a Novel Rearranged Version of the RETproto-Oncogene in a Human Thyroid Papillary Carcinoma». *Oncogene* 9 (2): 509–16.
- Shaw, George C., John J. Cope, Liangtao Li, Kenneth Corson, Candace Hersey, Gabriele E. Ackermann, Babette Gwynn, et al. 2006. «Mitoferrin Is Essential for Erythroid Iron Assimilation». *Nature* 440 (7080): 96–100.
- Sherr, C. J. 2000. «The Pezcoller Lecture: Cancer Cell Cycles Revisited». *Cancer Research* 60 (14): 3689–95.
- . 2004. «Living with or without Cyclins and Cyclin-Dependent Kinases». *Genes & Development* 18 (22): 2699–2711.
- Silvestri, Laura, Alessia Pagani, Antonella Nai, Ivana De Domenico, Jerry Kaplan, e Clara Camaschella. 2008. «The Serine Protease Matriptase-2 (TMPRSS6) Inhibits Heparin Activation by Cleaving Membrane Hemojuvelin». *Cell Metabolism* 8 (6): 502–11.
- Simons, Benjamin D., e Hans Clevers. 2011. «Strategies for Homeostatic Stem Cell Self-Renewal in Adult Tissues». *Cell* 145 (
- Sun, Jianlong, Azucena Ramos, Brad Chapman, Jonathan B. Johnnidis, Linda Le, Yu-Jui Ho, Allon Klein, Oliver Hofmann, e Fernando D. Camargo. 2014. «Clonal Dynamics of Native Haematopoiesis». *Nature* 514 (7522): 322–27.
- Vashchenko, Ganna, e Ross MacGillivray. 2013. «Multi-Copper Oxidases and Human Iron Metabolism». *Nutrients* 5 (7): 2289–2313.
- Verga Falzacappa, Maria Vittoria, Maja Vujic Spasic, Regina Kessler, Jens Stolte, Matthias W. Hentze, e Martina U. Muckenthaler. 2007. «STAT3

- Mediates Hepatic Heparin Expression and Its Inflammatory Stimulation». *Blood* 109 (1): 353–58.
- Vidal, Anxo, e Andrew Koff. 2000. «Cell-Cycle Inhibitors: Three Families United by a Common Cause». *Gene* 247 (1–2): 1–15.
- Wrighting, Diedra M., e Nancy C. Andrews. 2006. «Interleukin-6 Induces Heparin Expression through STAT3». *Blood* 108 (9): 3204–9.
- Yeh, S., e C. Chang. 1996. «Cloning and Characterization of a Specific Coactivator, ARA70, for the Androgen Receptor in Human Prostate Cells.» *Proceedings of the National Academy of Sciences* 93 (11): 5517–21.
- Yu, Yu, Zaklina Kovacevic, e Des R. Richardson. 2007. «Tuning Cell Cycle Regulation with an Iron Key». *Cell Cycle* 6 (16): 1982–94.
- Zhang, Caiguo. 2014. «Essential Functions of Iron-Requiring Proteins in DNA Replication, Repair and Cell Cycle Control». *Protein & Cell* 5 (10): 750–60.
- Zhang, Yan, Elise R. Lyver, Eiko Nakamaru-Ogiso, Heeyong Yoon, Boominathan Amutha, Dong-Woo Lee, Erfei Bi, et al. 2008. «Dre2, a Conserved Eukaryotic Fe/S Cluster Protein, Functions in Cytosolic Fe/S Protein Biogenesis». *Molecular and Cellular Biology* 28 (18): 5569–82.
- Zhao, Ningning, An-Sheng Zhang, e Caroline A. Enns. 2013. «Iron Regulation by Heparin». *The Journal of Clinical Investigation* 123 (6): 2337–43.